Permanent Magnets

Dr. Pelin Tozman

Functional Materials, Institute of Materials Science, Technische Universität Darmstadt, 64287 Darmstadt, Germany

pelin.tozman@tu-darmstadt.de

Learning outcomes:

TECHNISCHE UNIVERSITÄT DARMSTADT

Magnet development from Loadstone to NdFeB

Intrinsic magnetic properties: Magnetisation, Curie temperature
Anisotorpy field

Extrinsic magnetic propertis: Coercivity, Remanence,
Energy product

How to make a magnet, micsrostructure and performance relation

Discovery: First magnet

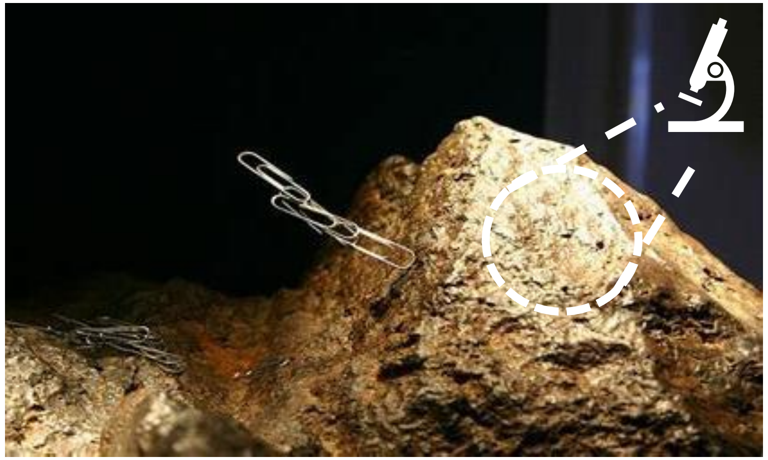

Lodestone: *Rocks rich in magnetite, Fe_3O_4, magnetized by huge electric current in lightining strikes*

Lightining Bolt: I= 10 kA to 200 kA

Ampere Law: $B = \frac{\mu_0 I}{2\pi r}$

$I = 30$ kA, $r = 1$m

$B = 6\ \mu T$

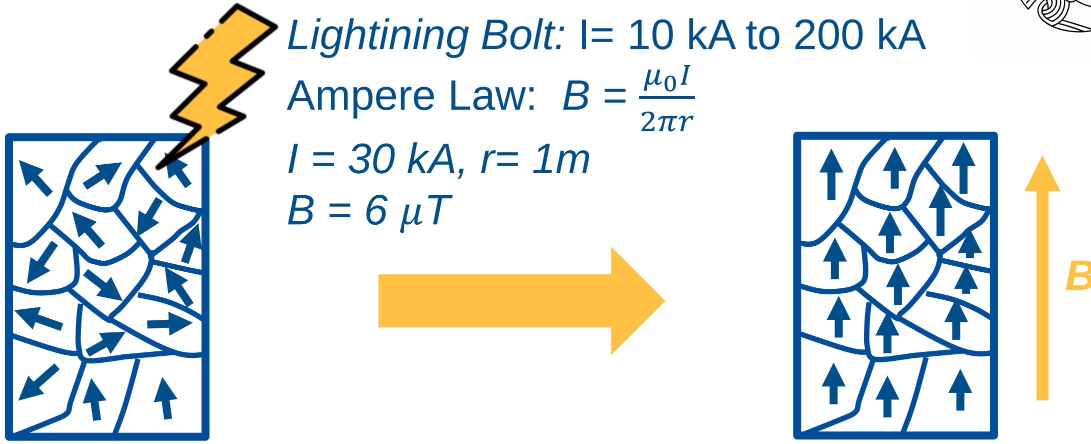

Domains randomly aligned unmagnetized

$\boldsymbol{B_{app}} = 0\ \ \boldsymbol{M} = 0$

No magnetostatic energy

Magnetized

$\boldsymbol{B_{app}} = 6\ \mu T\ \ \boldsymbol{M} = M_s$

magnetostatic energy

Magnetic materials consist of regions called **magnetic domains**, within which the magnetic moments of atoms are aligned.

A permanent magnet is a material that produces a magnetic field without the need for an external source of power or electric current.

Magnetization:

***H*-field:** Magnetic field strength **(A/m)**
***B*-field:** Magnetic flux density **(T)** **(**1 Oe = 10^{-4} T= 80 A/m)
B = μ_0(H+M) *Ampere law*
M **:** Magnetization **(A/m)**

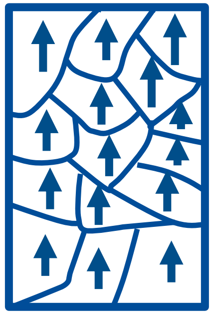

Permanent magnet
Have memory!

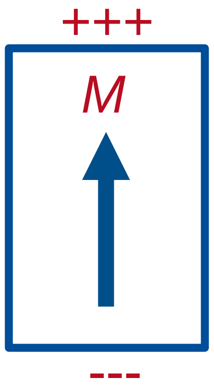

Normal component of M creates poles (∇.M ≠ 0)
→ H-field

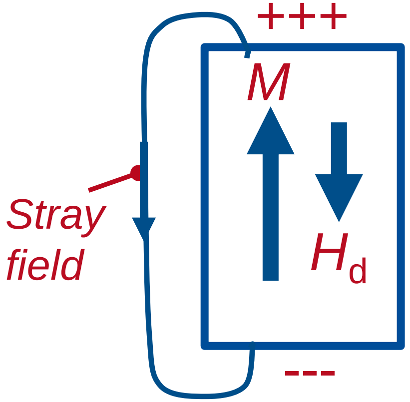

Demag field, H_d
$H_d = -\mathcal{N}M$

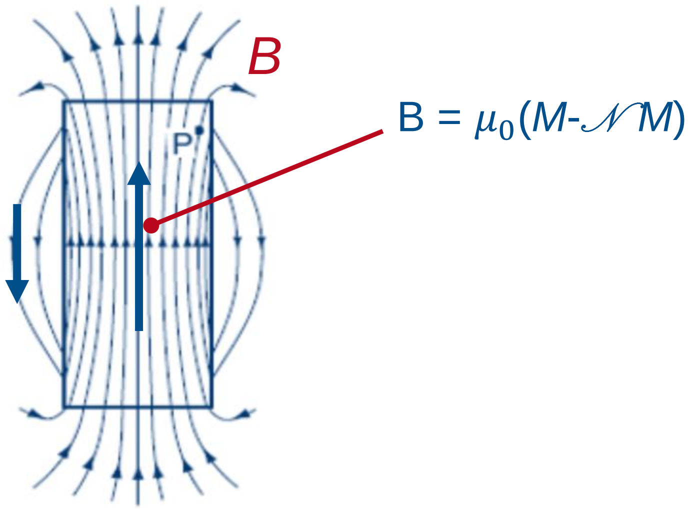

Gauss law ∇.*B* = 0
There is no magnetic monopole
Continous closed loop

Stray field: Equivalence of demagnetizing field in surrounding volume of a magnet
The magnetic flux density outside the magnet is the useful quantity for magnet applications.

[1] J. M. D. Coey, Journal of Physics: Condensed Matter 26, 064211 (2014).

Demagnetizing field: Magnetic tape

Shape	Direction		$\mathcal{N}$	
Long needle	// to axis	⊥ to axis	0	1/2
Thin film	// to axis	⊥ to axis	0	1
Sphere	Any direction		1/3	

[1] R. Skomski and J. M. D. Coey, Scripta Materialia 112, 3 (2016)

1928, Fritz Pfleumer

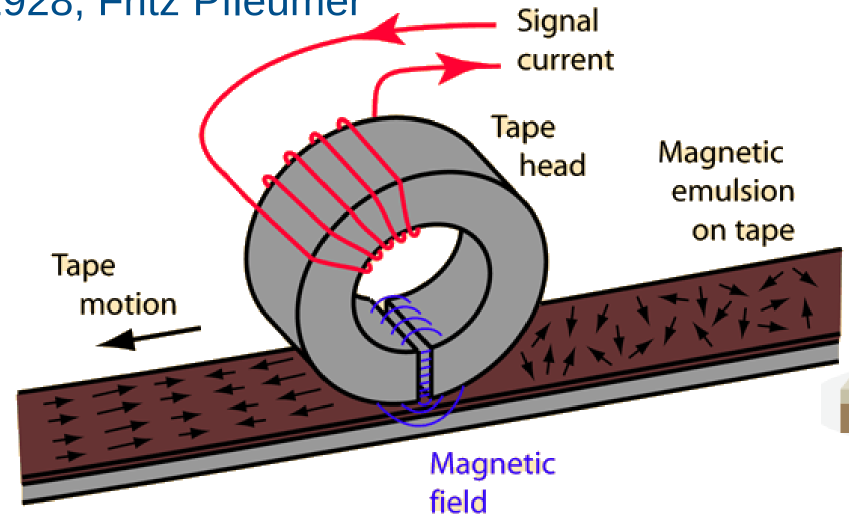

http://hyperphysics.phy-astr.gsu.edu/hbase/Audio/tape2.html

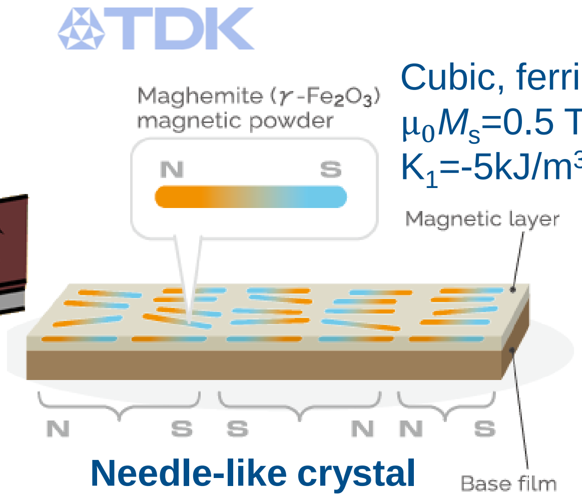

Cubic, ferrimagnet
$\mu_0 M_s$=0.5 T
K_1=-5kJ/m^3

Needle-like crystal

Writing:

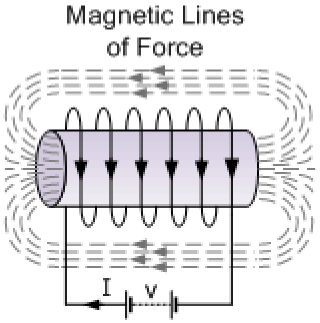

Electromagnetic induction

Applying AC current to the coil reverse the magnetization direction of the magnetic materials repeatedly

Reading:

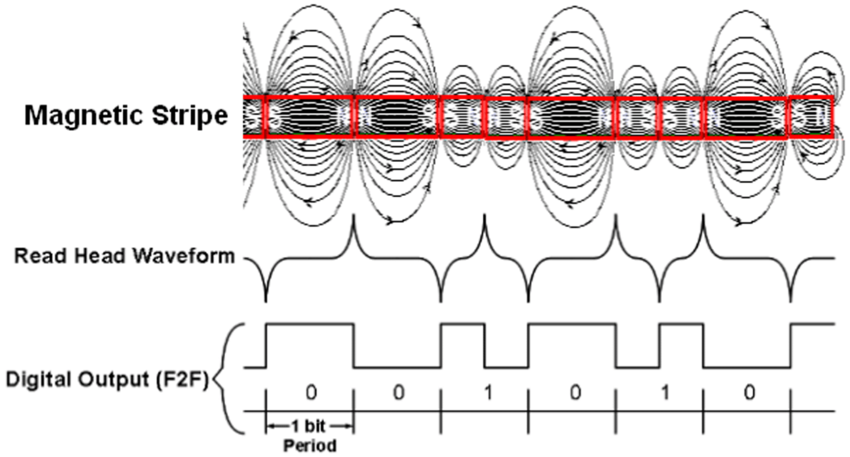

Demagnetizing field: AlNiCo

World's first artificial magnetic nanostructures
Developed: 1930–1970 (1931, T. Mishima) Doubled the performance of steel
AN under field ≈ 0.2 T Spinodal decomposition @800C of a quarternary cubic alloy → Neddle like nanoscale regions of ferromagnetic FeCo (α_1) needles embeded in non magnetix NiAl matrix (α_2).

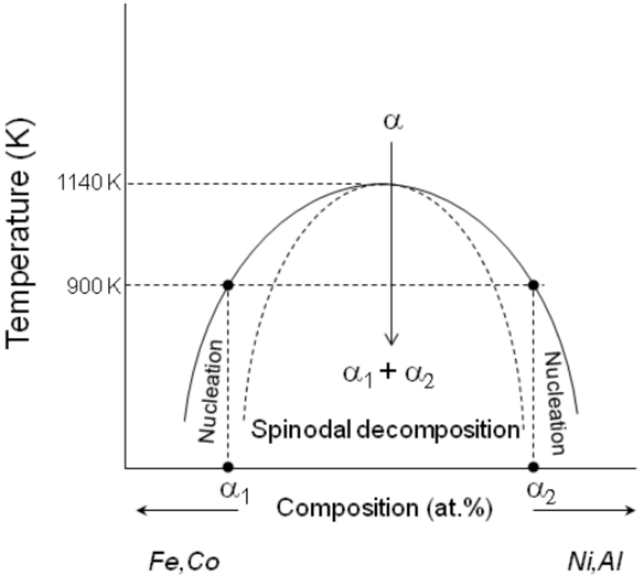

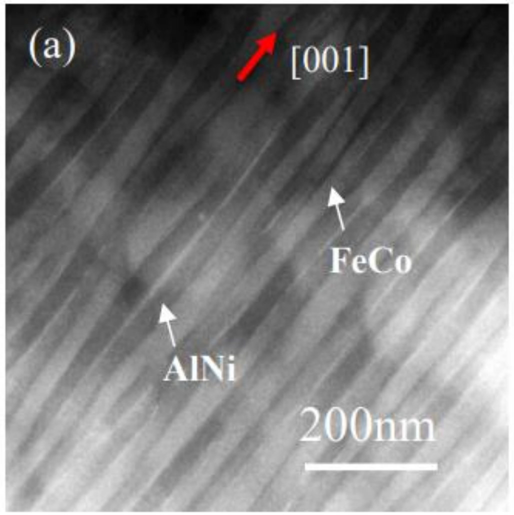

Cubic FeCo $\mathcal{N}$ = 0

Ideal case K_{shape} =1.2 MJ/m^3, K_1=20 kJ/m^3

$\mu_0 M_s$=2.45 T

$\mu_0 H_a$= $2K_{sh}/0.9\mu_0 M_s$ = 1.3 T

Does AlNiCo is an ideal Magnet?

Iwama Y. and Takeuchi M., Trans JIM 1974; 15, 371

L. Zhou et al. "Microstructure and coercivity in alnico 9, *Journal of Magn. and Magn. Mater.*471 (2019) 142-147.

Shape anisotropy

TECHNISCHE UNIVERSITÄT DARMSTADT

An ideal magnet should be prepared in any desired shape which means $H_c > M_s$
Shape anisotropy offer upper limit $H_c \approx M_s/2$ in ideal case. Shape is never enough!

$K_1^{shape} = ¼\mu_0 M_s^2(1 - 3\mathcal{N})$ For $\mathcal{N} = 0$, K_{shape} =1.2 MJ/m^3 $\mu_0 H_a$= 1.3 T

Alnico: High $T_c \approx$ 1200 K, $\mu_0 M_s \approx$ 0.6-1.4 T Low $\mu_0 H_c \approx$ 0.06 T -0.2T

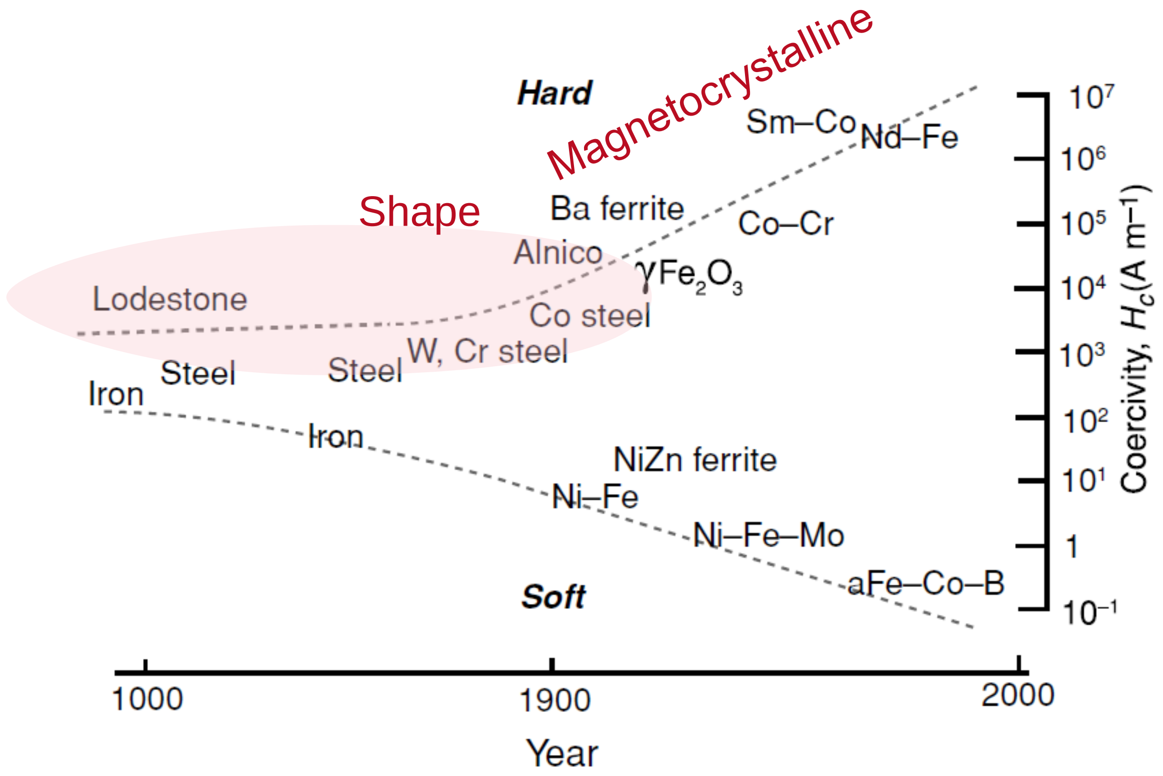

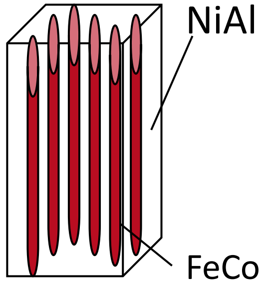

The seven ages of magnetism

Period	Dates	Icon	Drivers	Materials
Ancient period	-1500	Compass	State, geomancers	Iron, lodestone
Early modern age	-1820	Horshoe magnet	Navy	Iron, lodestone
Electromagnetic age	-1900	Electromagnet	Industry	Electric steel
Age of understanding	-1935	Pauli metrices	Academic	(AlNiCo)
High-frequency age	-1960	Magnetic resonance	Military	Ferrites
Age of applications	-1995	Electric screwdriver	Consumer market	Sm-Co, Nd-Fe-B
Age of spin electronics	-Present	Read head	Consumer market	Multilayers

Early Chinese Compass – 400 BC

Early telegraph system, Electric motor, compass, Magnetic seperator

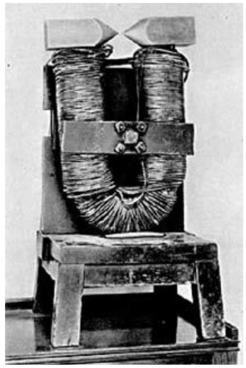

19th century electromagnet

Electric guitar pickup, high temperature applications in automative component, vintage audio equipment, precision instruments

Ferrite

1930

Dr. Y. Kato – Dr. T. Takei
Tokyo Institute of Technology

Hard  Soft

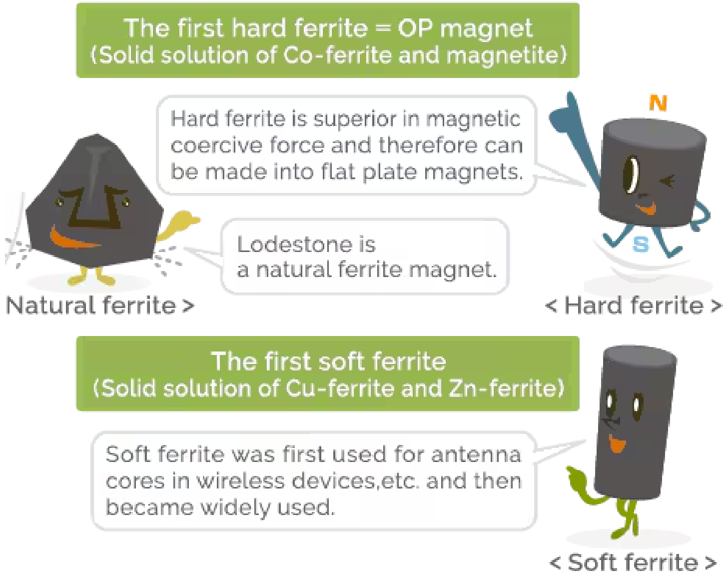

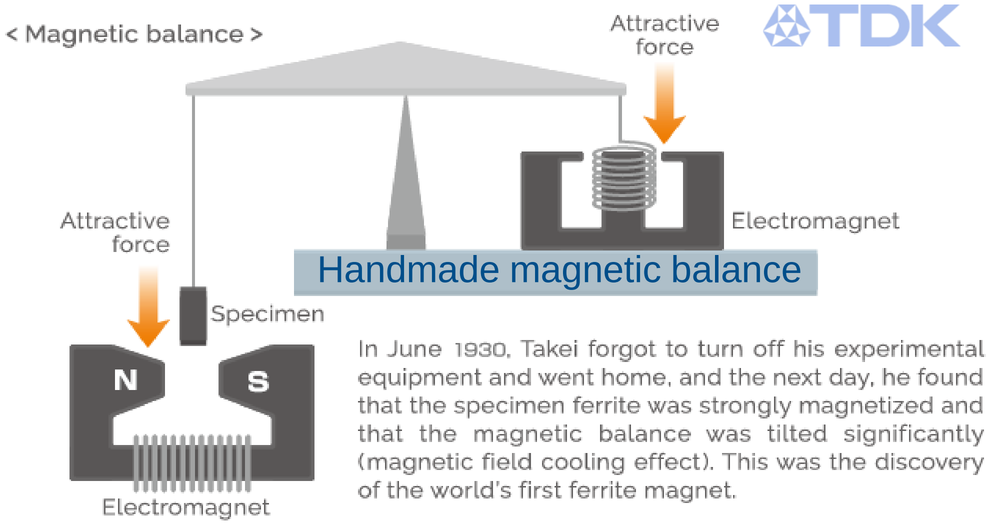

Measuring T_c, *M-T* up to 300ºC
Electromagnet remained applied → Cool down under field

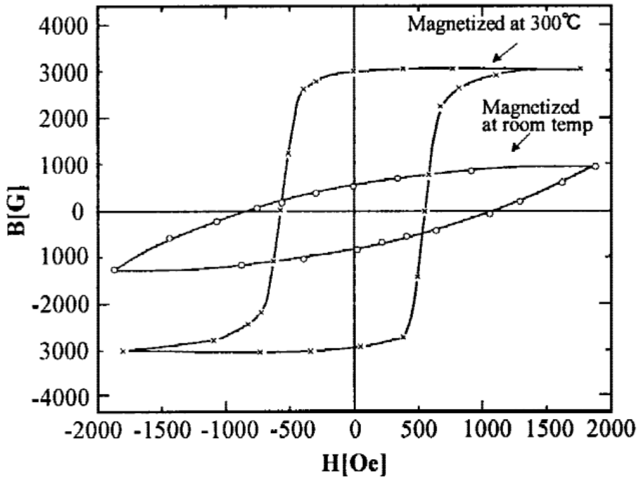

Fig. 2. Effect of magnetizing temperature on the hysteresis of a solid solution of $CoFe_2O_4$ and Fe_3O_4.

[1] M. Sugimoto, The past, present and future of ferrites, J. Am. Ceram. Soc. 82 (1999) 269-280

$CoFe_2O_4$, ferrimagnet:
Fm-3m, $\mu_0 M_s$ = 0.56T, K_1 = 290 kJ/m^3, $\mu_0 H_a$ = 1.3 T
Spin-orbit coupling associated with the Co^{2+} ions
Industrialized under the name “OP magnet”
(Ookayama’s permanent magnet) in 1935.

[2] JMD Coey, Magnetism and Magnetic materials, 2010, p.423

Ferrite

TECHNISCHE UNIVERSITÄT DARMSTADT

1930

Dr. Y. Kato – Dr. T. Takei
Tokyo Institute of Technology
Cubic Co-ferrite (semi hard)
Spin-orbit coupling Co^{2+} ions,
at octahedral sites of the spinel structure.

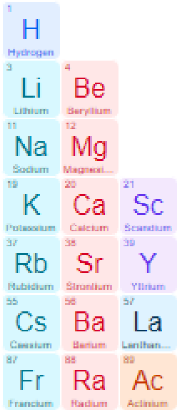

1951

Van Oosterhout based on Snoek work
Philips Research Laboratories
Hexagonal ferrite (hard) ferrimagnetic
Magnetocrystalline anisotropy
$MFe_{12}O_{19}$ M=Ba^{2+} (BaM) or Sr^{2+} (SrM)

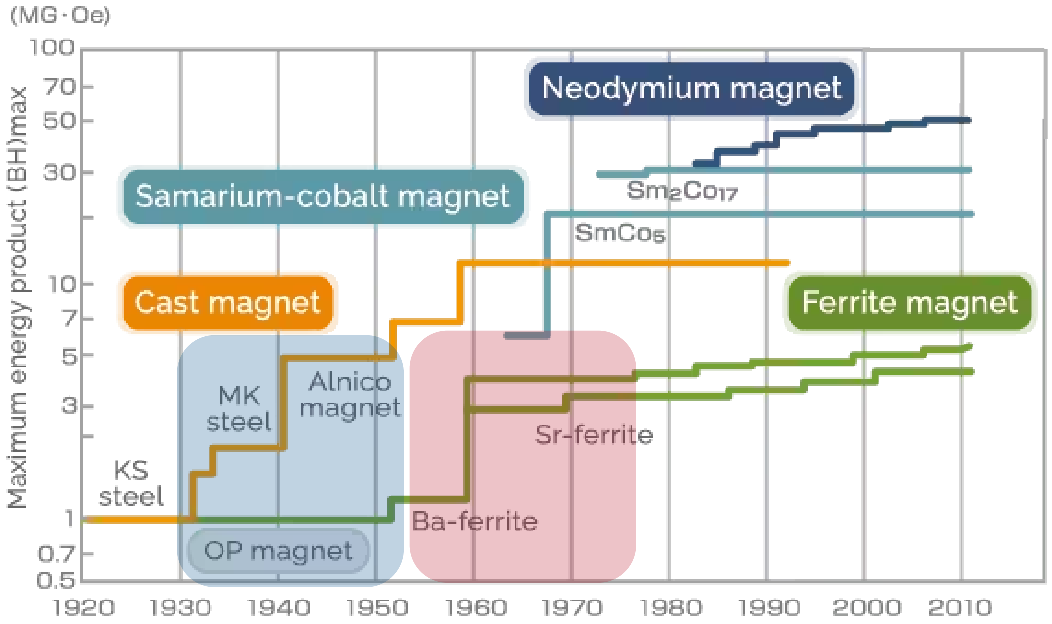

TDK

Hexagonal ferrite:The most produced magnet!

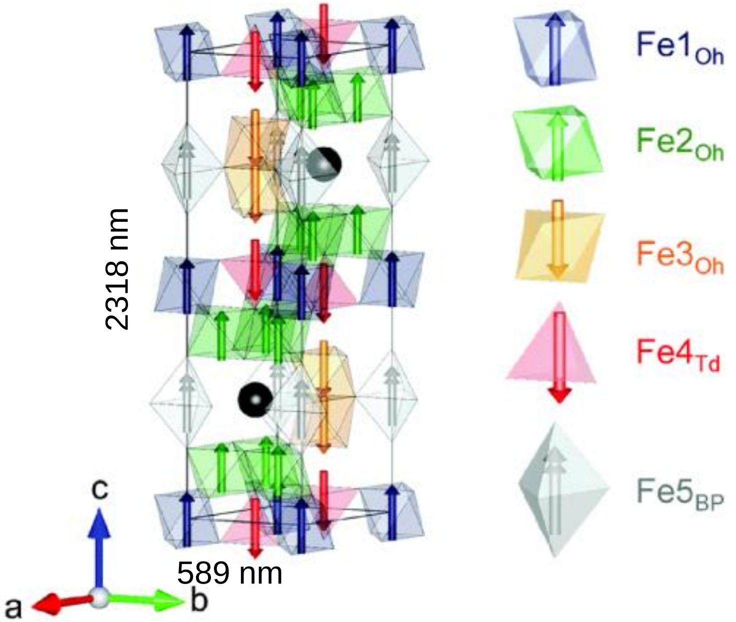

Figure 1. Representation of the crystal and magnetic structure of the M-type hexaferrites, i.e. $BaFe_{12}O_{19}$ and $SrFe_{12}O_{19}$. The black spheres represent the alkaline earth metals (Ba, Sr) while the colored polyhedra represent the five different Fe crystallograpic sites. The arrows represent the magnetic spins of the Fe atoms. Oxygen atoms

- Magnetocrystalline anisotropy → Hexagonal structure, spin-orbit coupling and local environment of Fe^{3+} ions.

M-type $MFe_{12}O_{19}$ M=Ba^{2+} or Sr^{2+}

Shape anisotropy is broken!!!
Large H_a with $H_c > M_s$
Freedom to magnetic circuit designer

But Ferrimagnetic largely composed of O_2 → M_s is poor

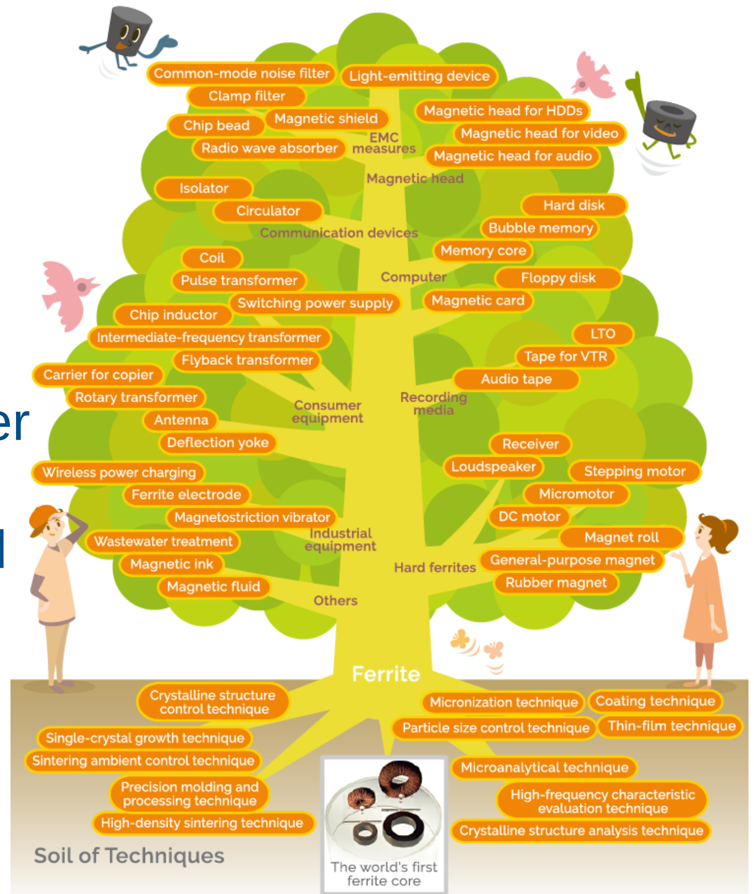

Application: Fridge magnet, motors, actuators, sensors and holding devices

[1] C. Granados-Miralles et al. On the potential of hard ferrite ceramics for permanent magnet technology—a review on sintering strategies, J. Phys. D Appl. Phys. 54, (2021) 303001.

Rare earth based magnets:

1966
First RE magnet YCo_5
Strant and Hoffer
Hexagonal $SmCo_5$
Huge H_a from Sm 4f electron

1970s
Sm_2Co_{17} magnets
Strant, Senno-Taware, TDK
Rhombohedral, Larger M_s
Practical application
$Sm(Co_{bal}Fe_{0.245}Cu_{0.07}Zr_{0.02})_{7.8}$

1980s
$Nd_2Fe_{14}B$
Kuz‘ma crystal structure
Croat melt spun ribbons
Sagawa NdFeB magnet

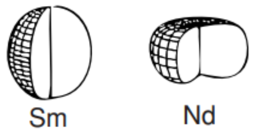

Charge density distribution

Material	$\mu_0 M_s$ (T)	$\mu_0 H_a$ (T)	T_c (K)	$(BH)_{max}$ (kJ/m^3)
Ba ferrite	**0.48**	**0.1**	**740**	**39**
$SmCo_5$	**1.07**	**40**	**1020**	**240**
YCo_5	**1.07**	**13**	**987**	**227**
Sm_2Co_{17}	**1.28**	**5.6**	**838**	**326**
$Nd_2Fe_{14}B$	**1.61**	**7.6**	**588**	**510**

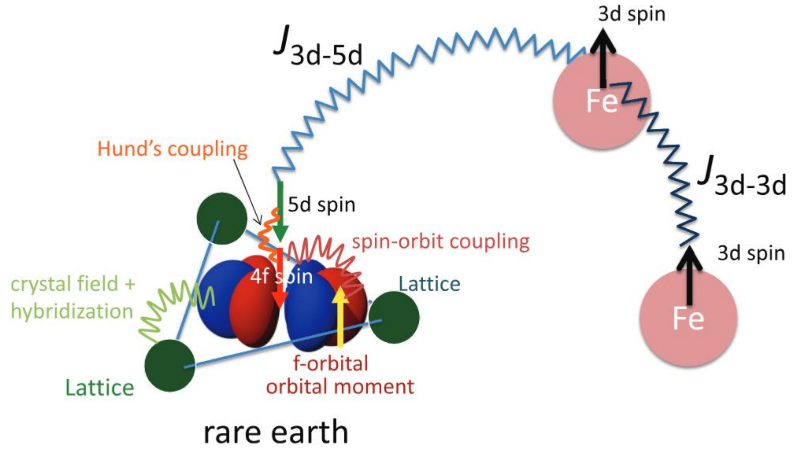

RE: High H_a
TM: High T_c, M_s

$$(BH)_{MAX} = \frac{1}{4}\mu_0 M_s^2$$

[1] J. M. D. Coey, Hard magnetic materials: A perspective, IEEE Trans. on magn. (2011) 4671-81
[2] T. Miyake et al., Understanding and optimization of hard magnetic compounds from first principles, *STAM,* 22 (2021) 543-556

Nowadays magnets:

TECHNISCHE UNIVERSITÄT DARMSTADT

Global magnet market

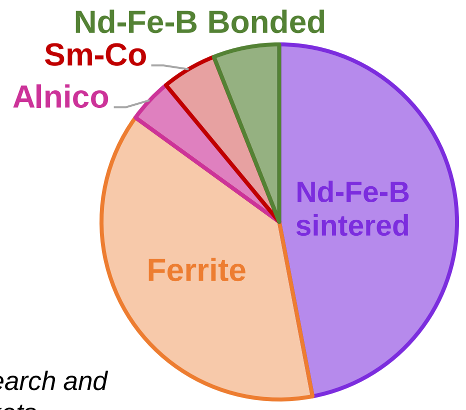

Research and Markets

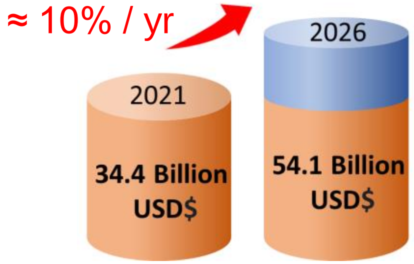

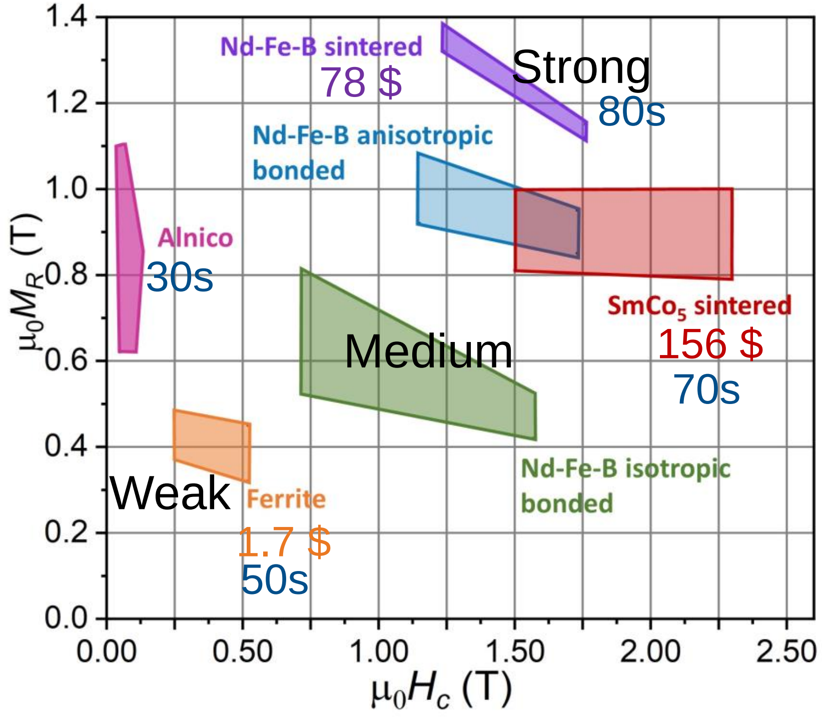

Green application

Mobility

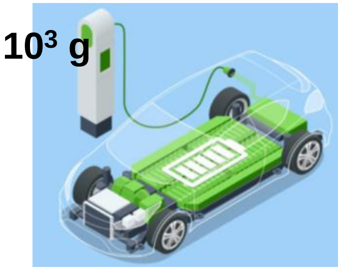

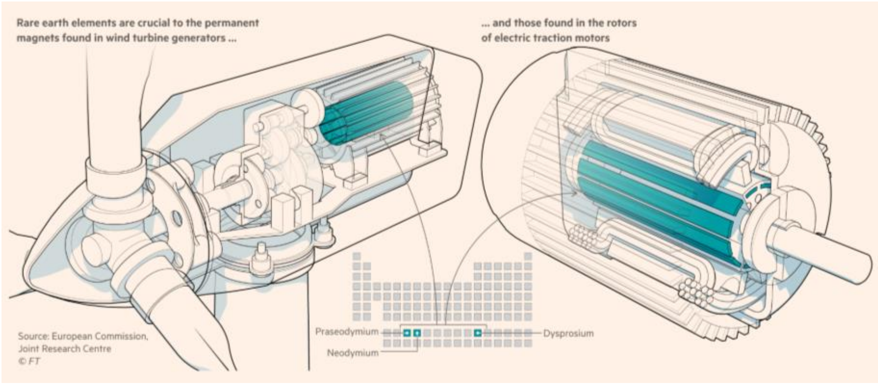

Additive Dy, Tb

Magnet stability at elevated temperature ≈200°C

[1] J.M.D. Coey, Engineering, 6, 119-131, 2020

[2] O. Gutfleisch, Adv. Mater. 23, 821-842, 2011

Magnet recipe:

TECHNISCHE UNIVERSITÄT DARMSTADT

Intrinsic magnetic properties

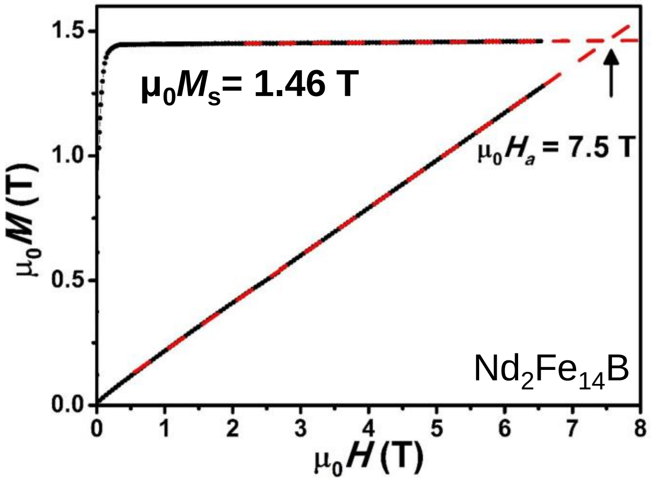

High anisotropy (H_a)
Magnetization (M_s)
Curie temperature (T_c)

Atomic and crystal structure

Material	$\mu_0 M_s$ (T)	$\mu_0 H_a$ (T)
$Nd_2Fe_{14}B$	**1.61**	**7.6**
Ferrite	**0.48**	**0.1**

+

Microstructure

Intergranular phase

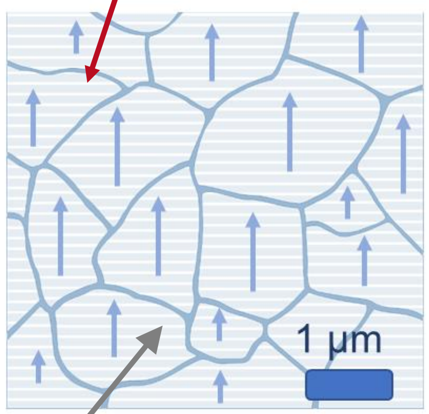

Fine magnetic grains isolated with intergranular phase

Nd-Fe-B
Phase diagram

Hard
Magnetic
$Nd_2Fe_{14}B$

Low melting
point phase

→

Extrinsic magnetic properties

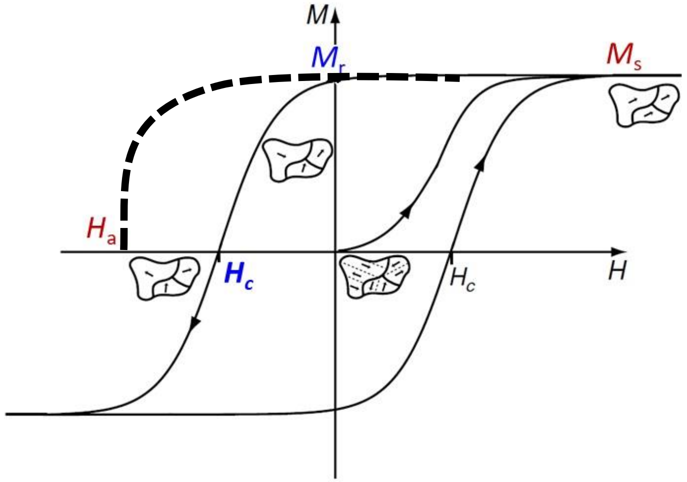

High coercivity (H_c) and remanence (M_r)

Nd-Fe-B
Ferrite

Magnetocrystalline anisotropy:

Spin-orbit coupling and crystal field interaction → Field tends to stabilize particular orbitals and spin-orbit interactions align magnetic moments in principal axes of crystal

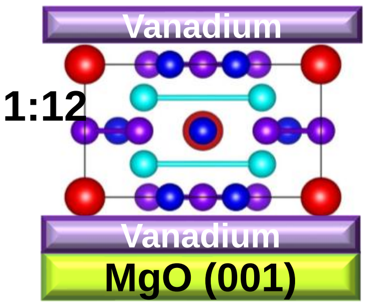

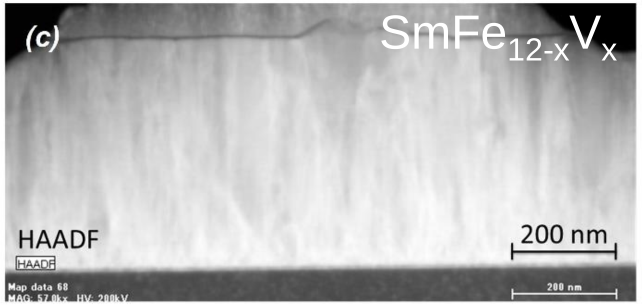

Material	$\mu_0 M_s$ (T)	$\mu_0 H_a$ (T)	T_c (K)
$SmFe_{12}$	**1.64**	**12**	**555**
$Nd_2Fe_{14}B$	**1.61**	**7.6**	**588**

[1] P. Tozman et al., Acta Mater. 232 (2022) 117928
[2] Y. Hirayama et al., Scr. Mater., 138 (2017), pp. 62-65

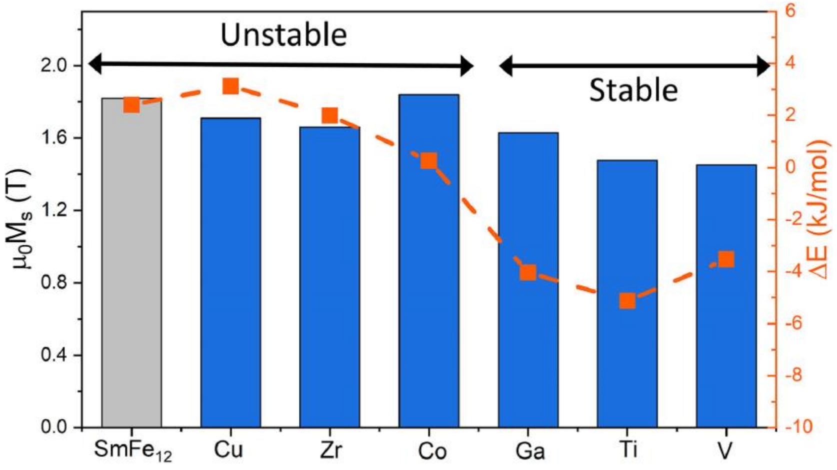

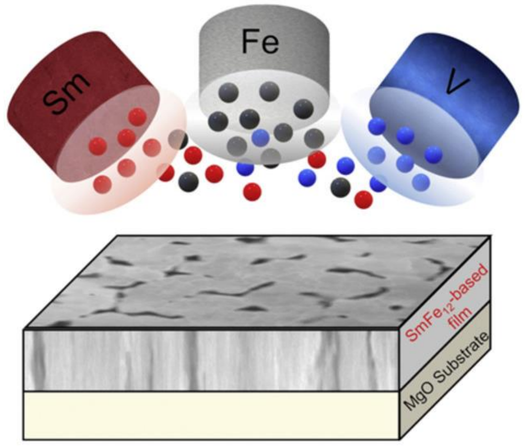

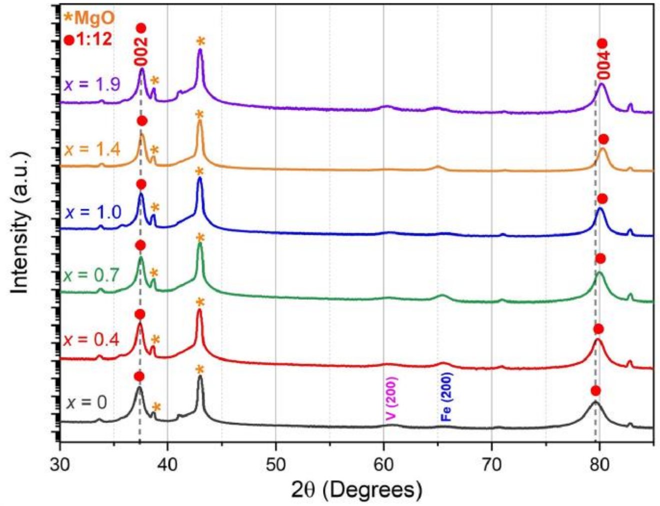

Magnetocrystalline anisotropy: $SmFe_{11-x}V_x$

(1) Cross point

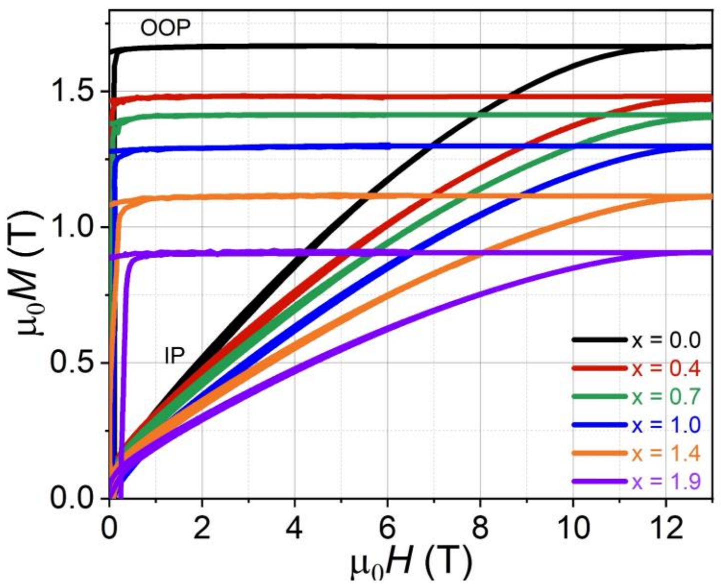

(2) Torque curve

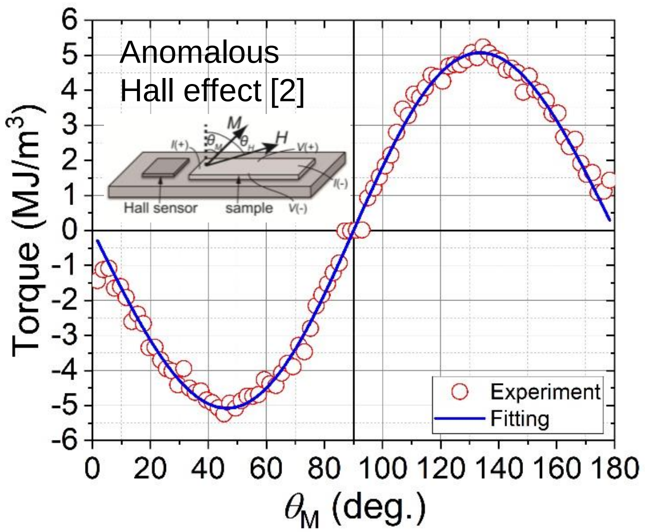

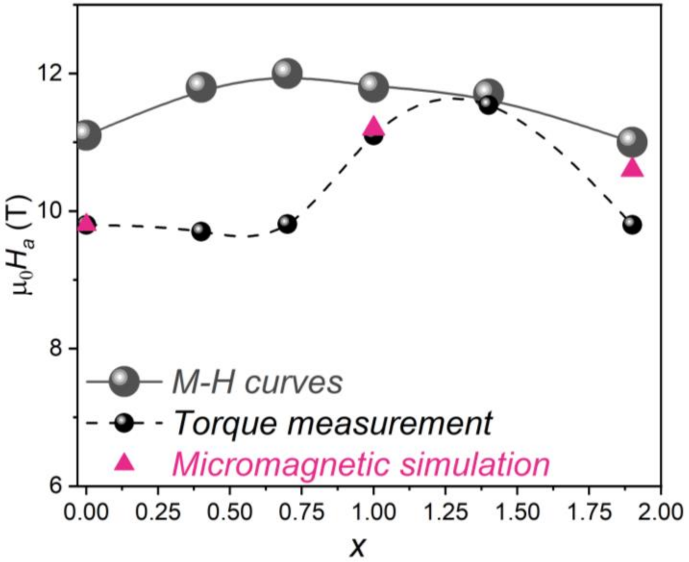

(3) Micromagnetic modelling

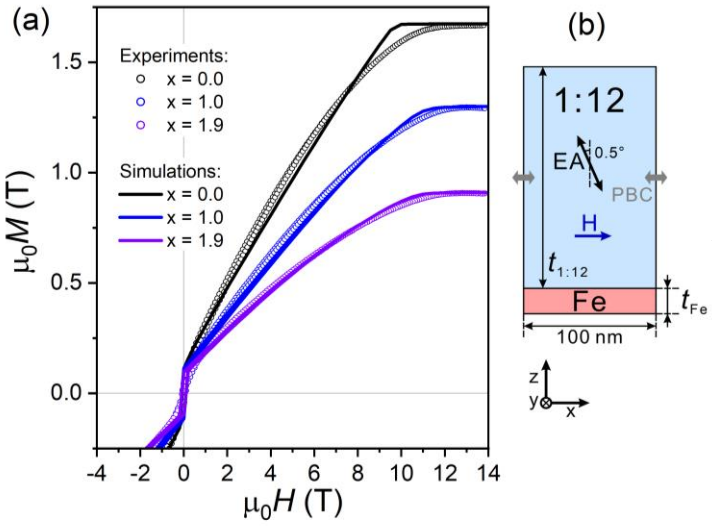

α-Fe
$\mu_0 M_s$ = 2.15 T ,
A = 21 pJ/m
1:12:
Exp. M_s , K_1 and K_2 ,
A =7.2 pJ/m

[1] P. Tozman et al., Acta Mater. 232 (2022) 117928
[2] T. Ono et al., Appl. Phys. Exp. 11 (2018) 033002.

Curie temperature

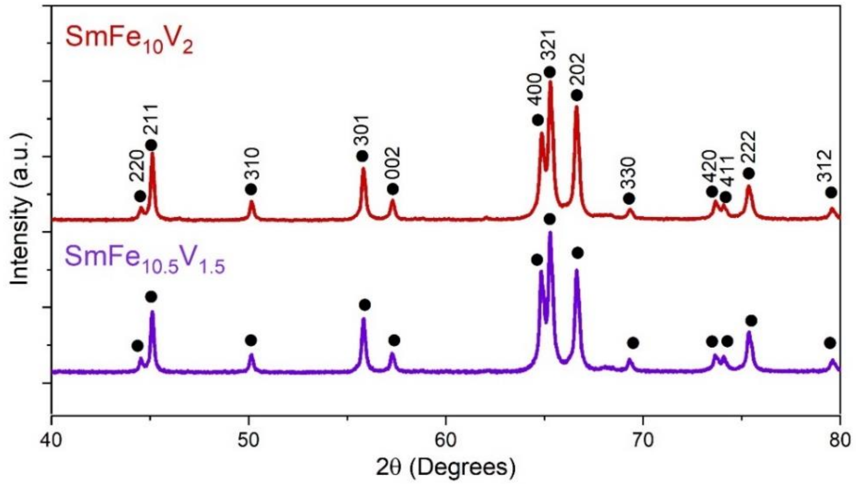

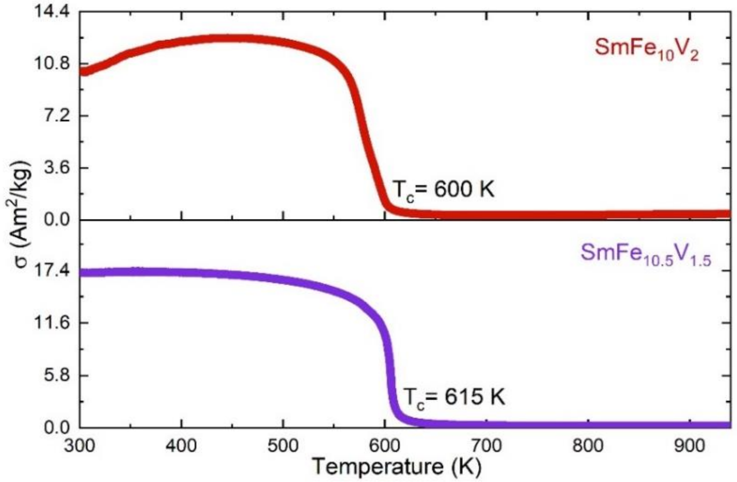

[1] M.D. Kuz'min, Phys. Rev. Lett. 94 (2005) 107204.
[2] P. Tozman et al., Acta Mater. 232 (2022) 117928

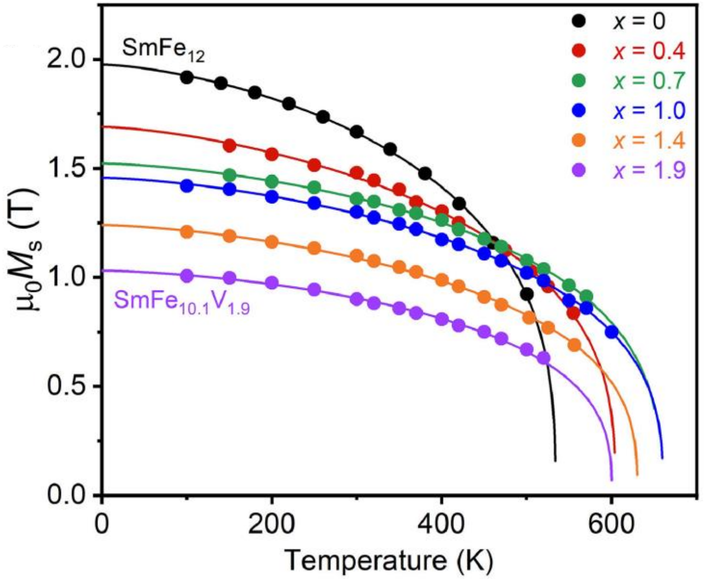

T_c → Least square fitting [1].

$$M_S(T) = M_S(0)\left[1 - s\left(\frac{T}{T_C}\right)^{\frac{3}{2}} - (1-s)\left(\frac{T}{T_C}\right)^{\frac{5}{2}}\right]^{\frac{1}{3}}$$

$M_s(0)$, T_c and s (shape parameter) are constant

$$s = 0.176\frac{g\mu_B}{M_S(0)}\left(\frac{k_B T_C}{D}\right)^{\frac{3}{2}}$$

D is spin wave stiffness

Hardness parameter κ

The criterion that a magnet can be fabricated in any shape without demagnetizing itself may be formulated in terms of the magnetic hardness parameter of the material defined as

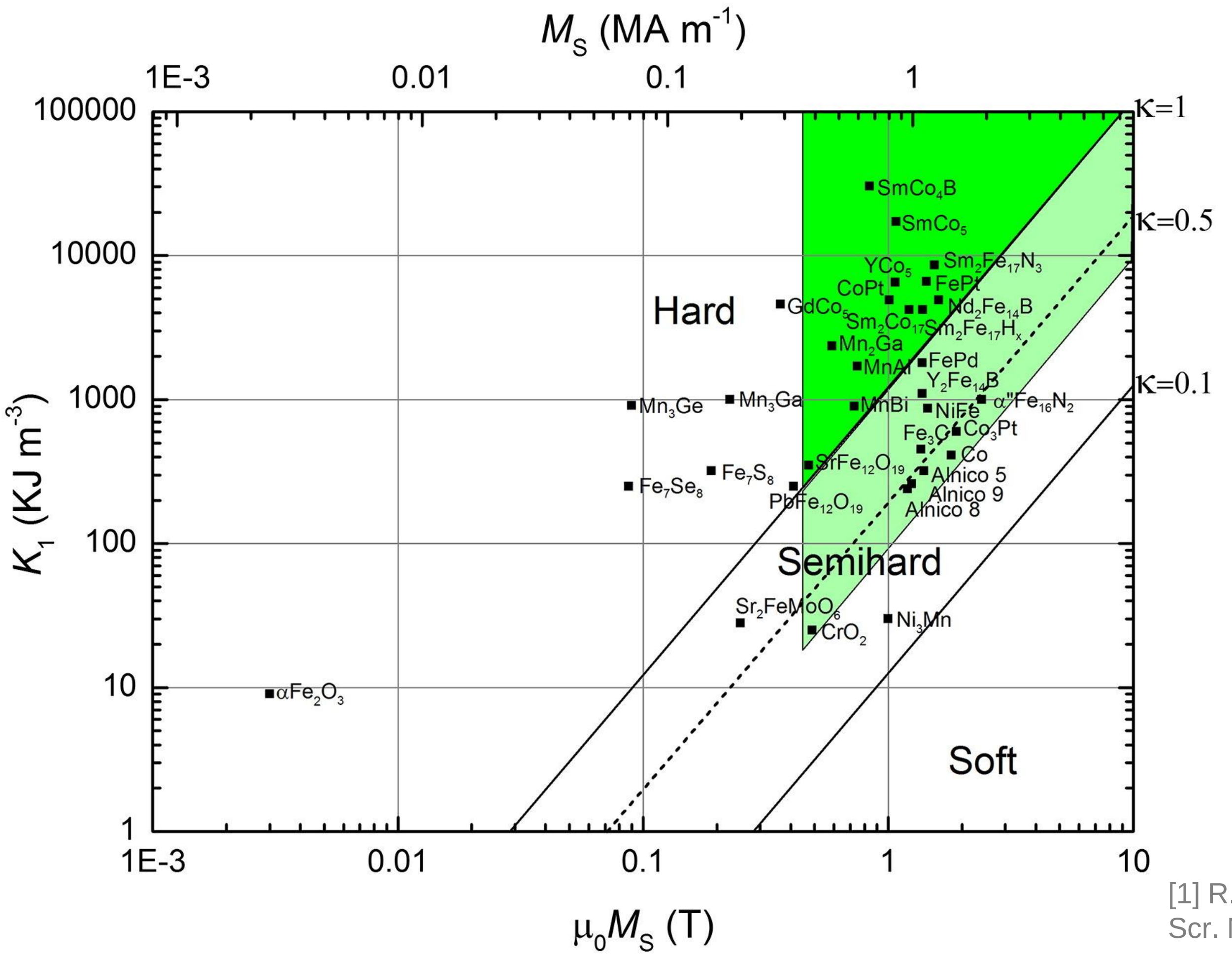

$$\kappa = \sqrt{K_1/\mu_0 M_s^2}$$

K > 1 Permenant magnet

Hard region: K > 1 Efficient magnet in any shape

Semihard materials in the pale green area can be used to make oriented magnets with a severely shape-limited energy product.

[1] R. Skomski, J. M. D. Coey, Magnetic anisotropy- How much is enough for a permanent magnet?, Scr. Mater., 112, (2016) 3-8.

Magnet recipe:

Intrinsic magnetic properties

High anisotropy (H_a)
Magnetization (M_s)
Curie temperature (T_c)

+

Microstructure

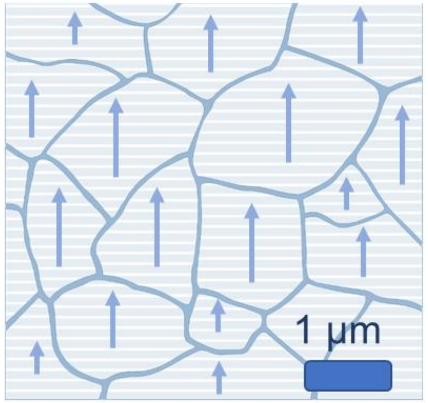

Fine magnetic grains isolated with intergranular phase

→

Extrinsic magnetic properties

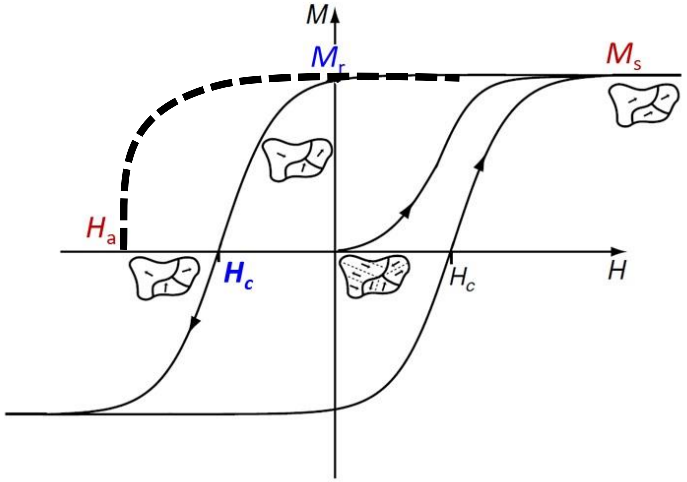

High coercivity (H_c) and remanence (M_r)

Why we need such microstructure to develop coercivity?
How we can obtain such microstructure?

Why we need such microstructure to generate coercivity?

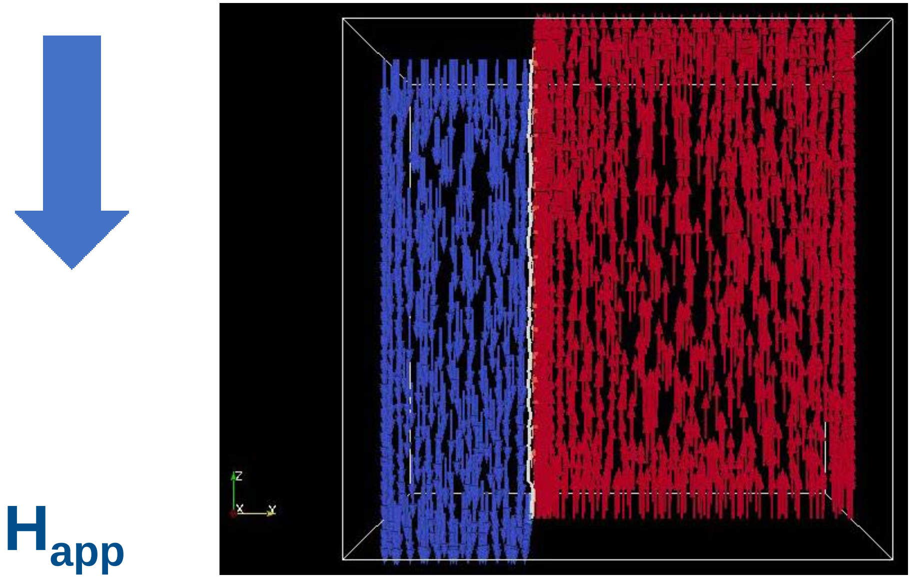

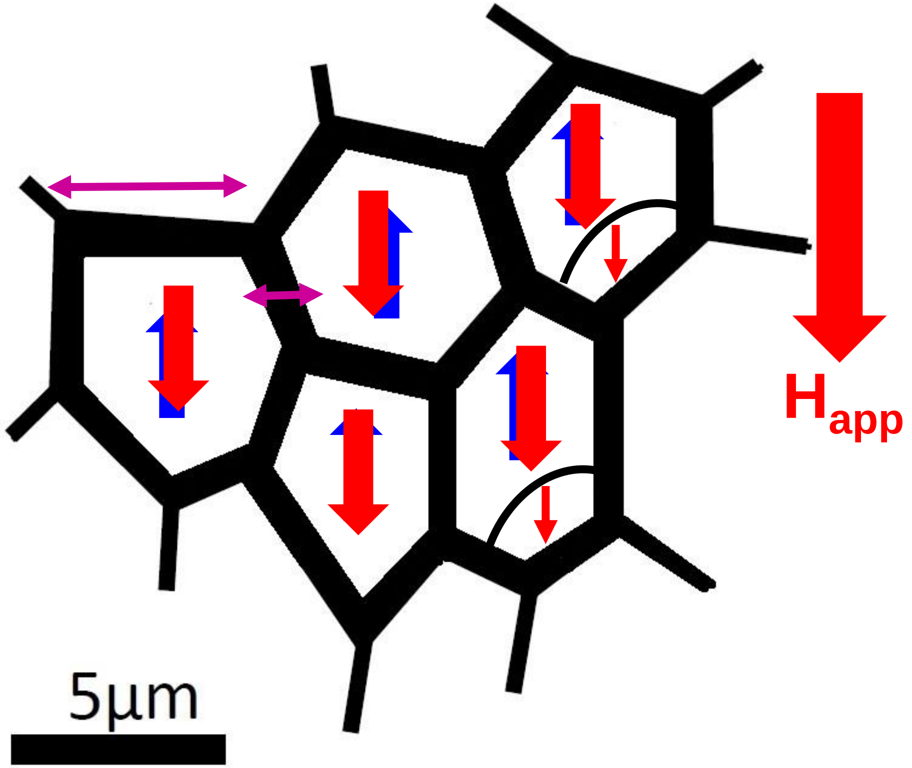

Nucleation type: Creation of a reverse domain and associated domain wall at the position where the energy barrier is lowest.

Hard magnets: Key parameters

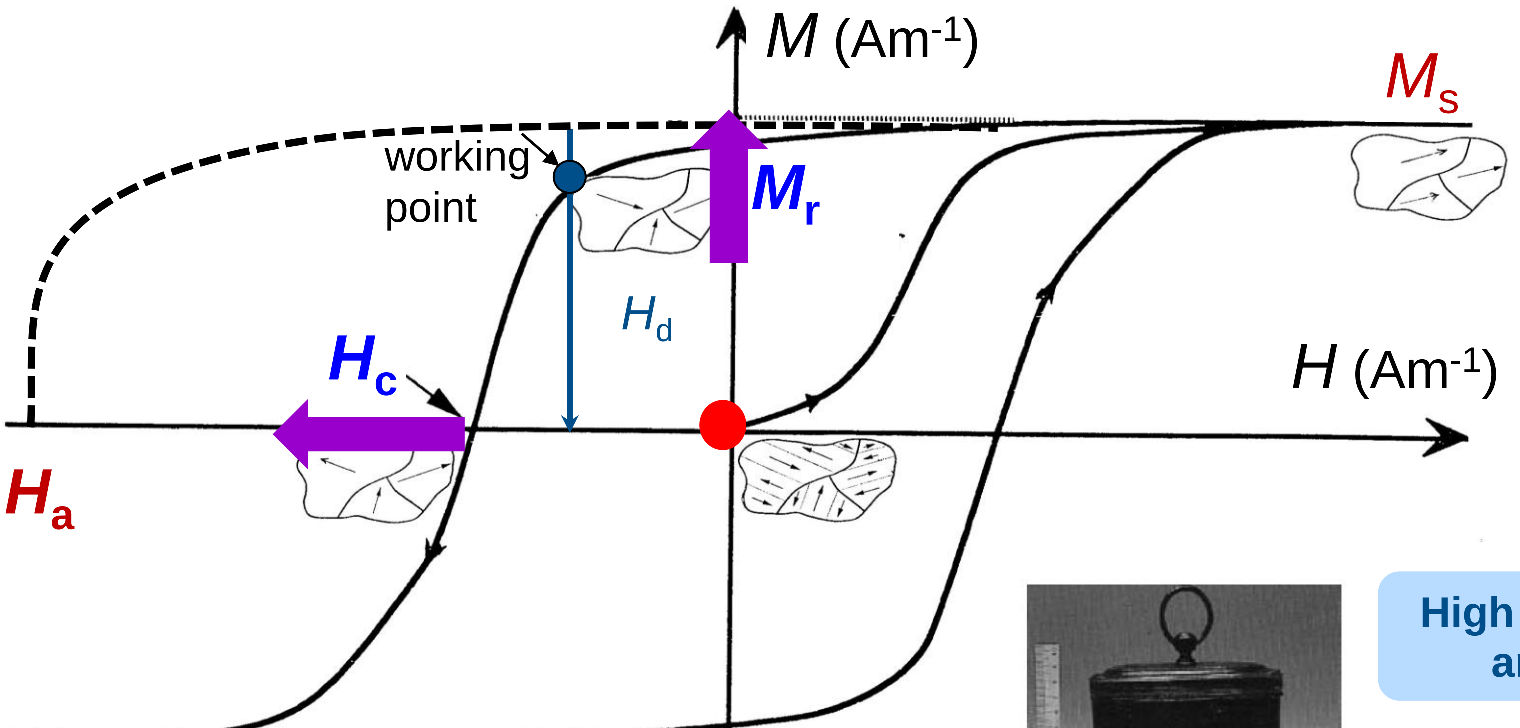

[1] J. M. D. Coey, IEEE Trans. on Magn., 47, 12, 2011

An early eighteenth century lodestone, a ferrite magnet (right) and a Nd–Fe–B magnet (front), which all store about a joule of energy.

High coercivity ($H_c \approx 0.2$–$0.3H_a$) and remanence ($M_r \leq M_s$)

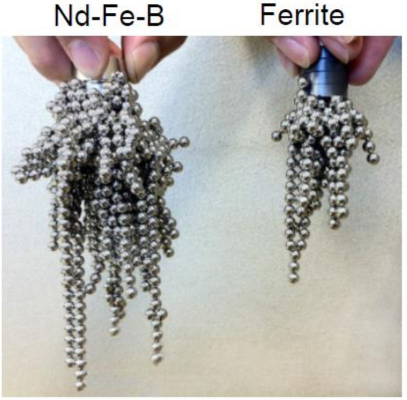

Sample subject only its H_d

Microstructure effect on $(BH)_{max}$:

$Nd_2Fe_{14}B$ $\mu_0 M_s = 1.6$ T

Anisotropic magnet

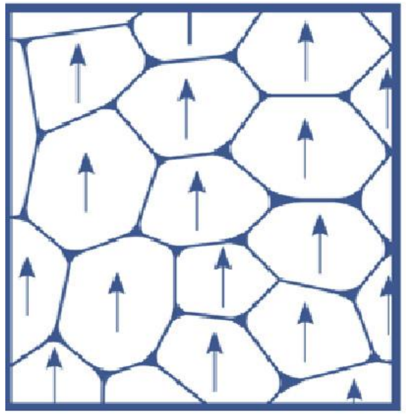

Sintered magnet
Highly oriented grains minimum volume nonmagnetic intergranular

$(BH)_{MAX} = \frac{1}{4} \mu_0 M_s^2$
$= 515$ kJ/m³

Efficiency: 100%

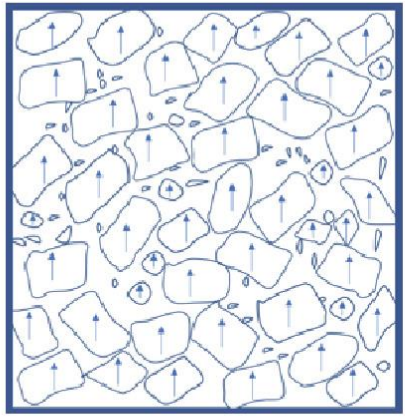

Oriented bonded magnet
Magnetic grains are embedded in a polymer (30%)

$(BH)_{MAX} = \frac{1}{4} f^2 \mu_0 M_s^2$
$= 252$ kJ/m³

Efficiency: 70%

Isotropic magnet

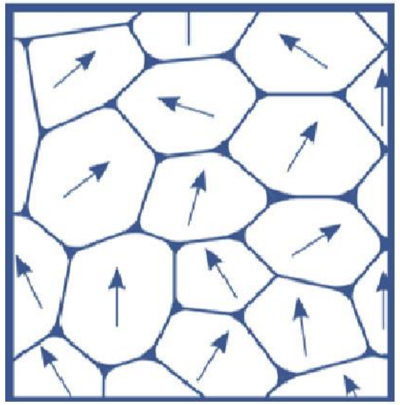

Randomly oriented Grains
<Mz>=Ms/2

$(BH)_{MAX} = 1/16 \mu_0 M_s^2$
$= 129$ kJ/m³

Efficiency: 25%

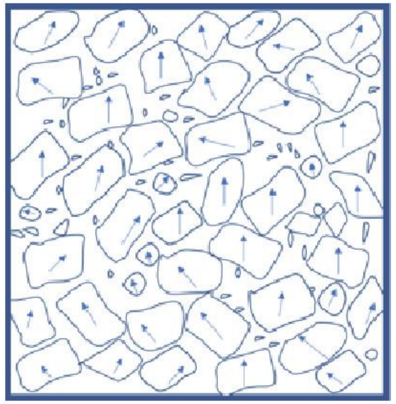

Randomly oriented Bonded
Compression or injection molding

$(BH)_{MAX} = 1/16 f^2 \mu_0 M_s^2$
$= 63$ kJ/m³

Efficiency: 18%

Processing routes:

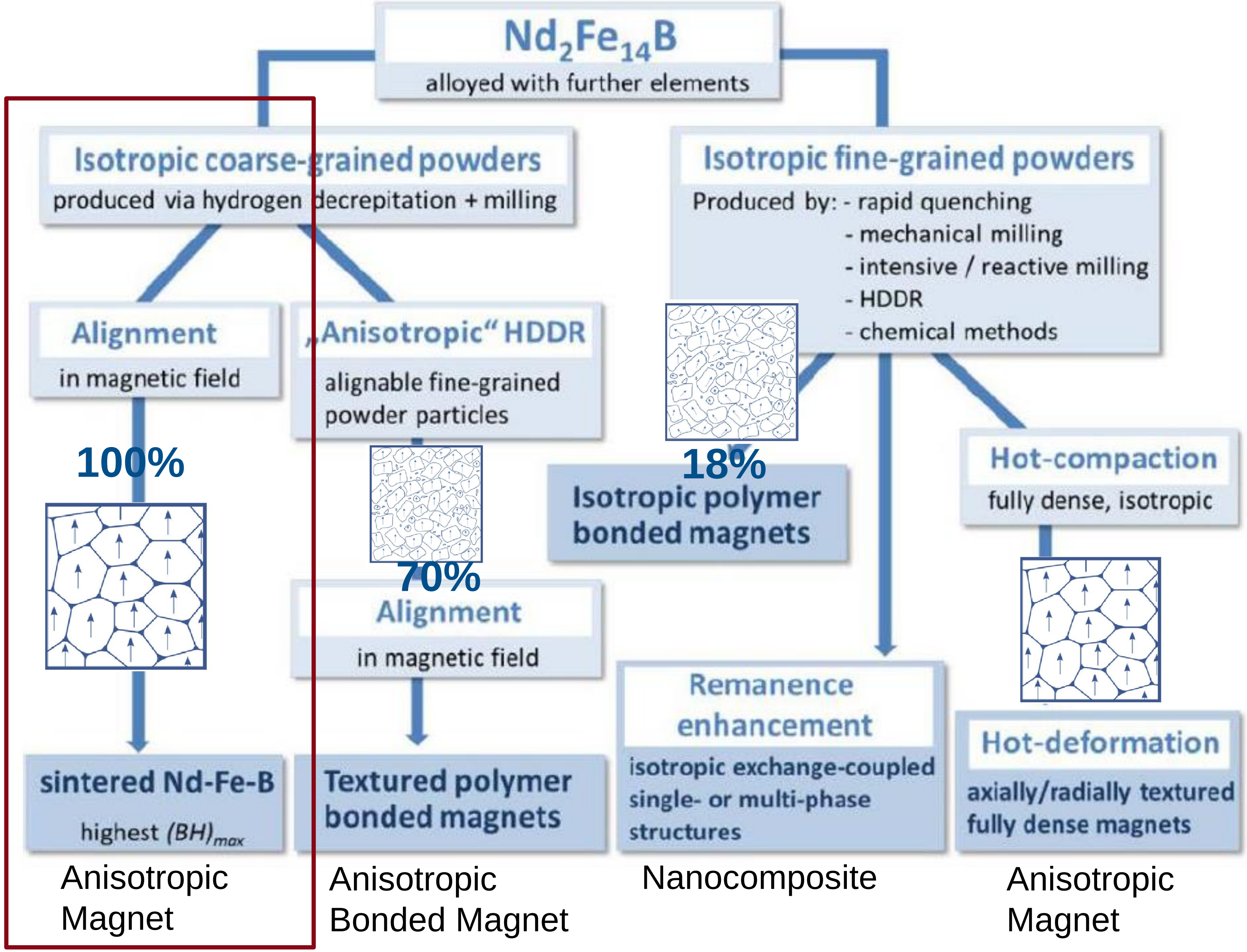

K.-H. Müller, S. Sawatzki, R. Gauss and O. Gutfleisch, Handbook of Magnetism and Magnetic Materials. Cham: Springer International Publishing, 2021, ed. by J.M.C. Coey and S. Parkin,

Microstructure: NdFeB sintered magnet

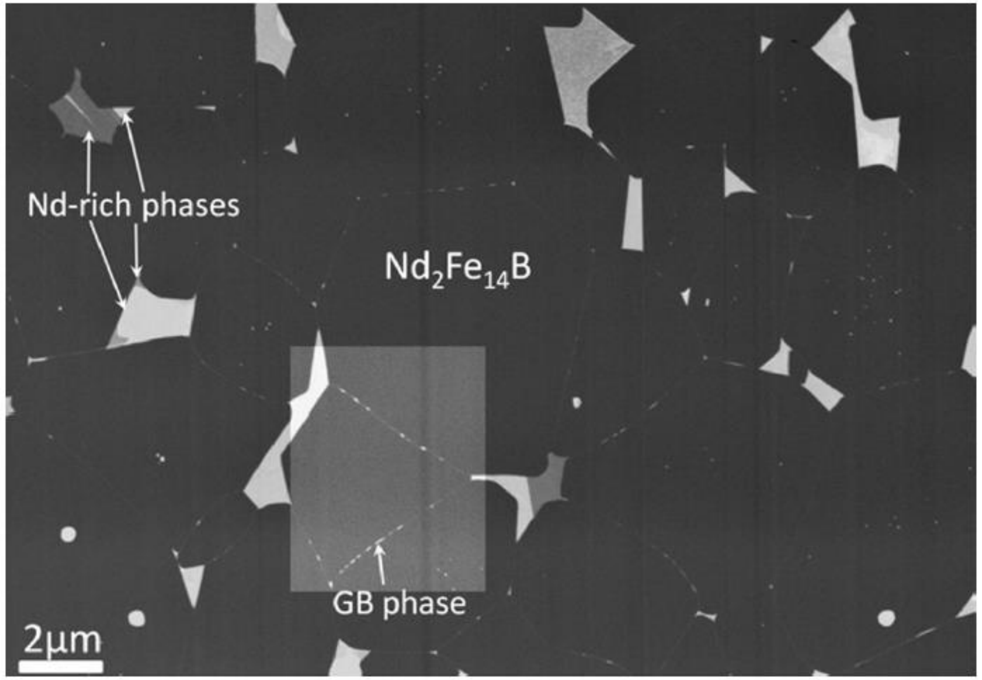

K. Hono, T. Ohkubo, H. Sepehri-Amin, J. Jpn. Inst. Metals 76 (2012)

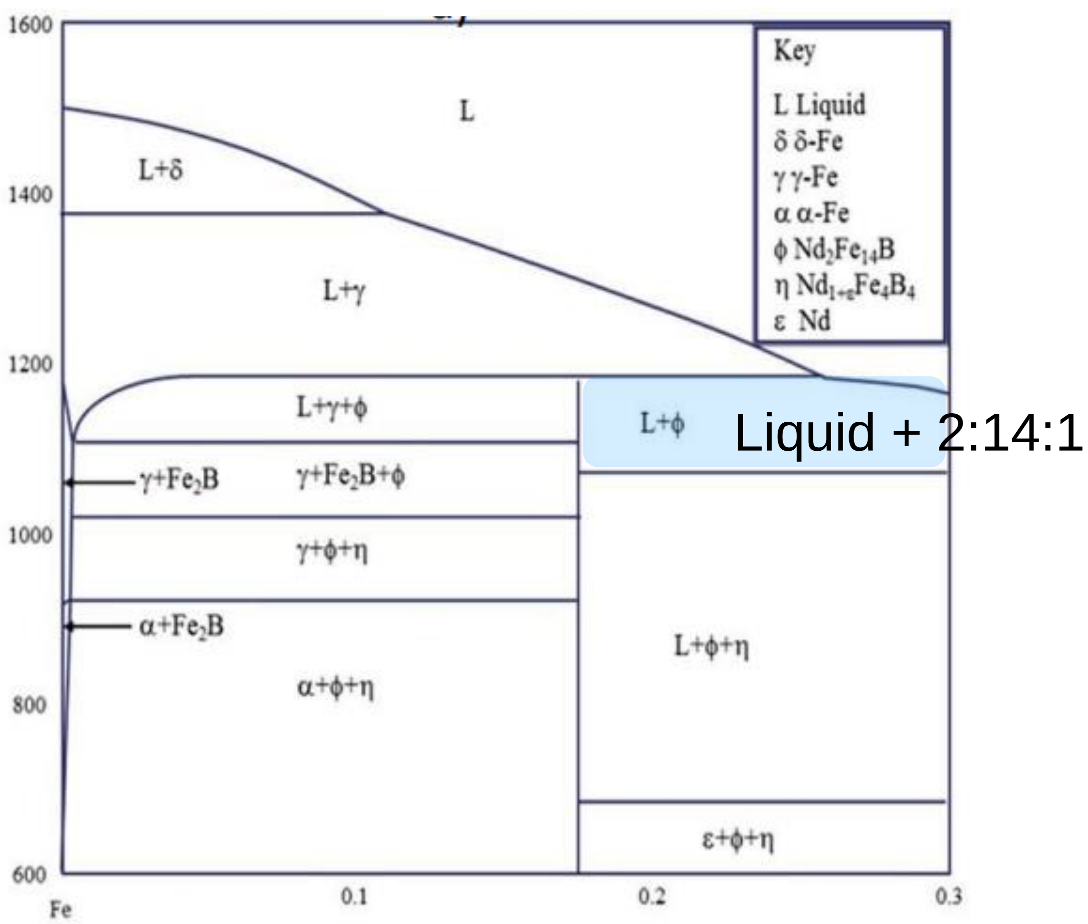

Microstructure: NdFeB sintered magnet

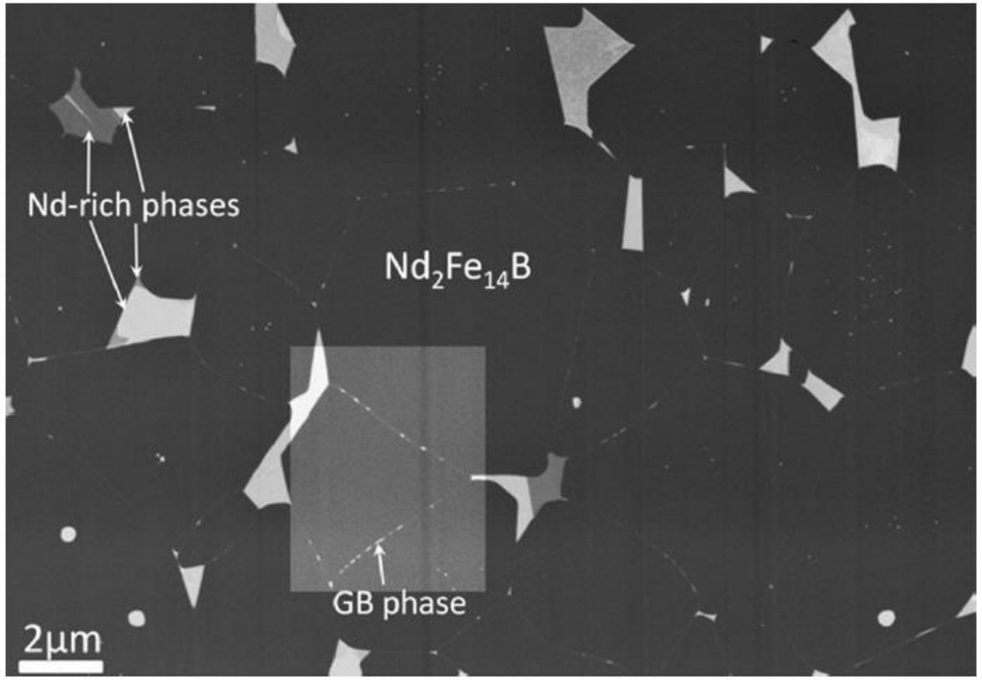

K. Hono, T. Ohkubo, H. Sepehri-Amin, J. Jpn. Inst. Metals 76 (2012)

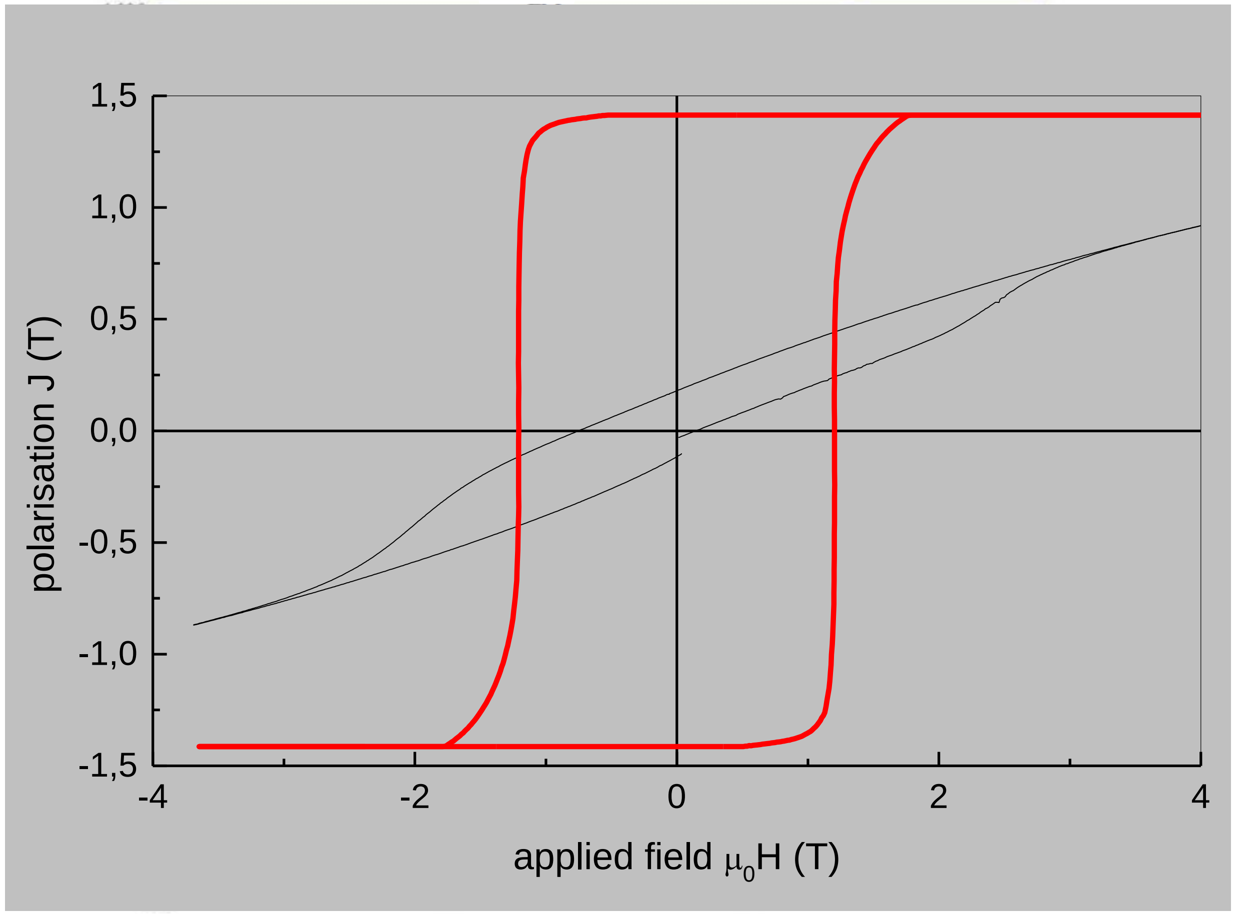

Nd-Fe-B sintered magnet

TECHNISCHE UNIVERSITÄT DARMSTADT

Ingredients

Raw materials: Nd,Fe,B

Melting

Induction, Arc Melting

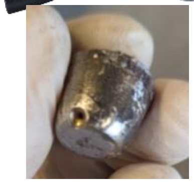

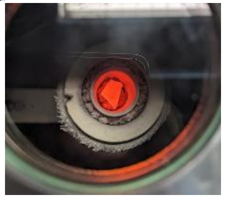

Strip casting

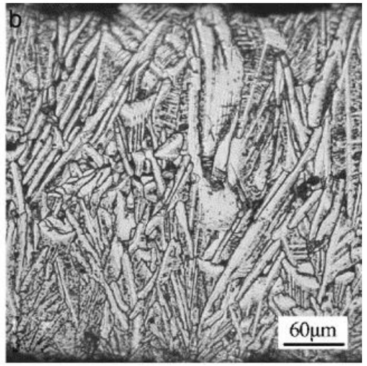

Grain size refinement

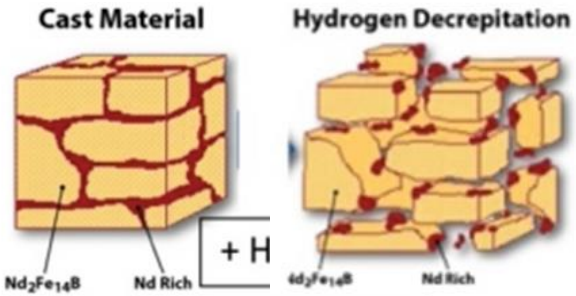

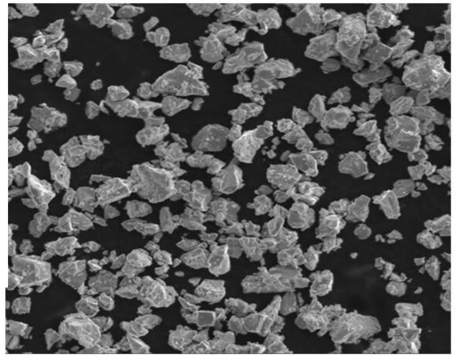

SDM Magnetics

Hydrogen Decrepitation and Jet milling

→ Single crystal powder particles 3-5 um

Pressing in magnetic field

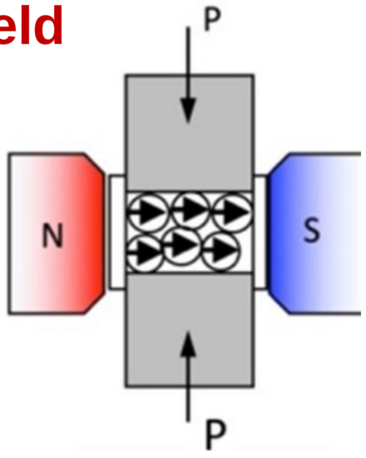

Sintering / Heat treatment/ Magnetizing

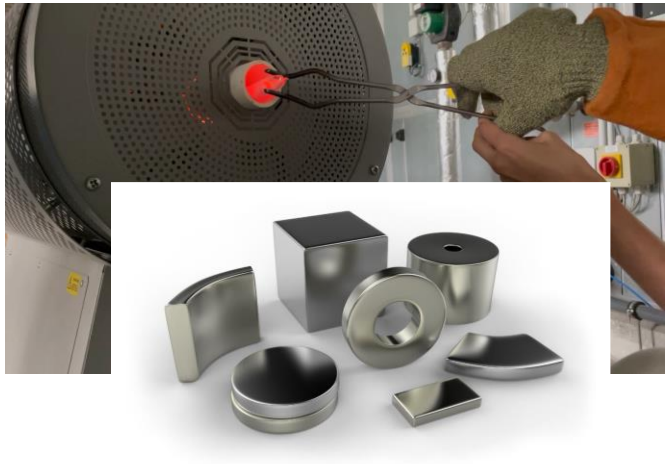

Expectation versus reality:

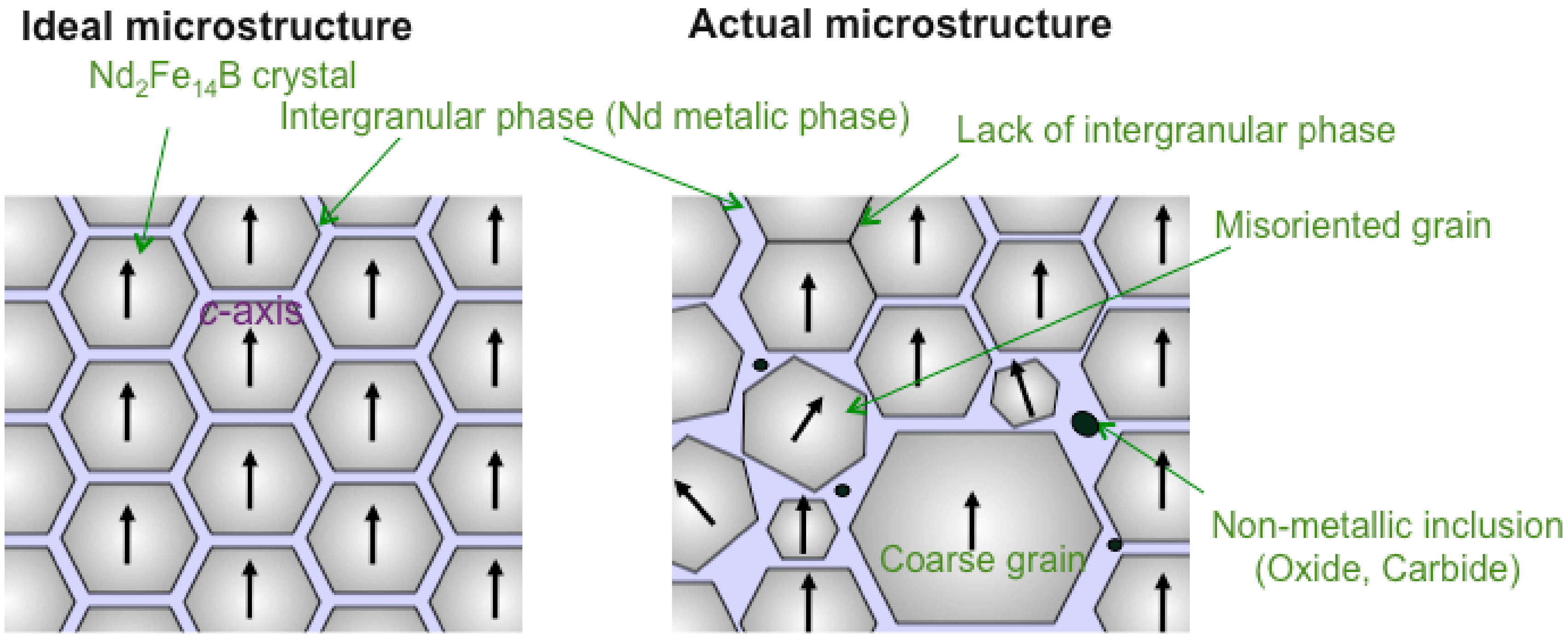

- Fine (~sub-micron size) and uniform $Nd_2Fe_{14}B$ crystal grains
- Perfect orientation
- Nd metallic phase covers all $Nd_2Fe_{14}B$ crystal grains

- Lack of Nd metallic phase → Lower coercivity
- Non-metallic inclusion → Lower coercivity
- Misoriented grain → Lower squareness
- Coarse grain → Lower coercivity

1987 SSMC $(BH)_{max}$=405 kJ/m^3 B_r=1.46 T H_c =736 kA/m
2005 NEOMAXX $(BH)_{max}$ =474 kJ/m3 B_r=1.555T H_c =653 kA/m

Anisotropic powders: HDDR

Hydrogen-disproportionation (HD) process and a Desorption-recombination (DR) process

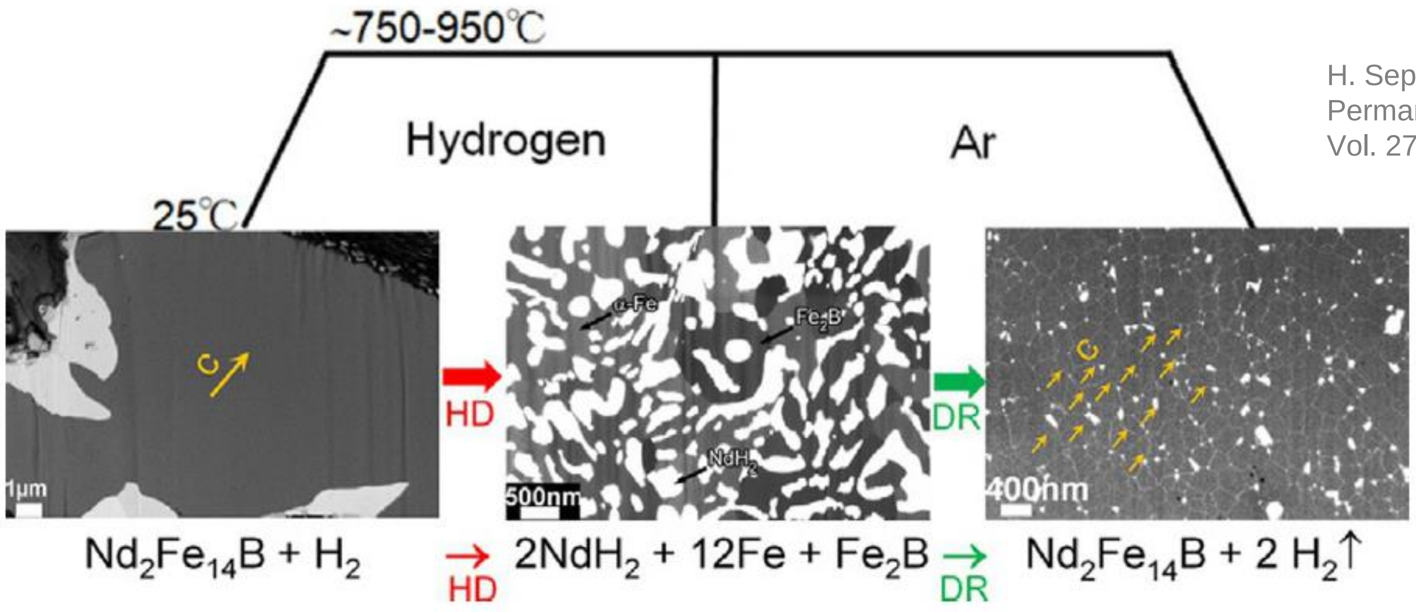

Nanosize powders

H. Sepehri-Amin et al., Advances in Nd-Fe-B Based Permanent Magnets, Handbook of Magnetic Materials, Vol. 27 (2020)

FIG. 4 Schematic of hydrogenation disproportionation desorption recombination process of Nd-Fe-B based powders.

- Starts: Mono-crystalline 2:14:1 powders prepared crushed ingot
- HD: Nd rich grain boundary absorbs H → forms NdH_2 → volume expension →Bulk material decrepitate → Single-crystalline nanosized powders
- DR: Powders AN in Ar to recombines all these phases → ultra fined grained $Nd_2Fe_{14}B$.

Anisotropic powders: HDDR

Hydrogen-disproportionation (HD) process and a Desorption-recombination (DR) process

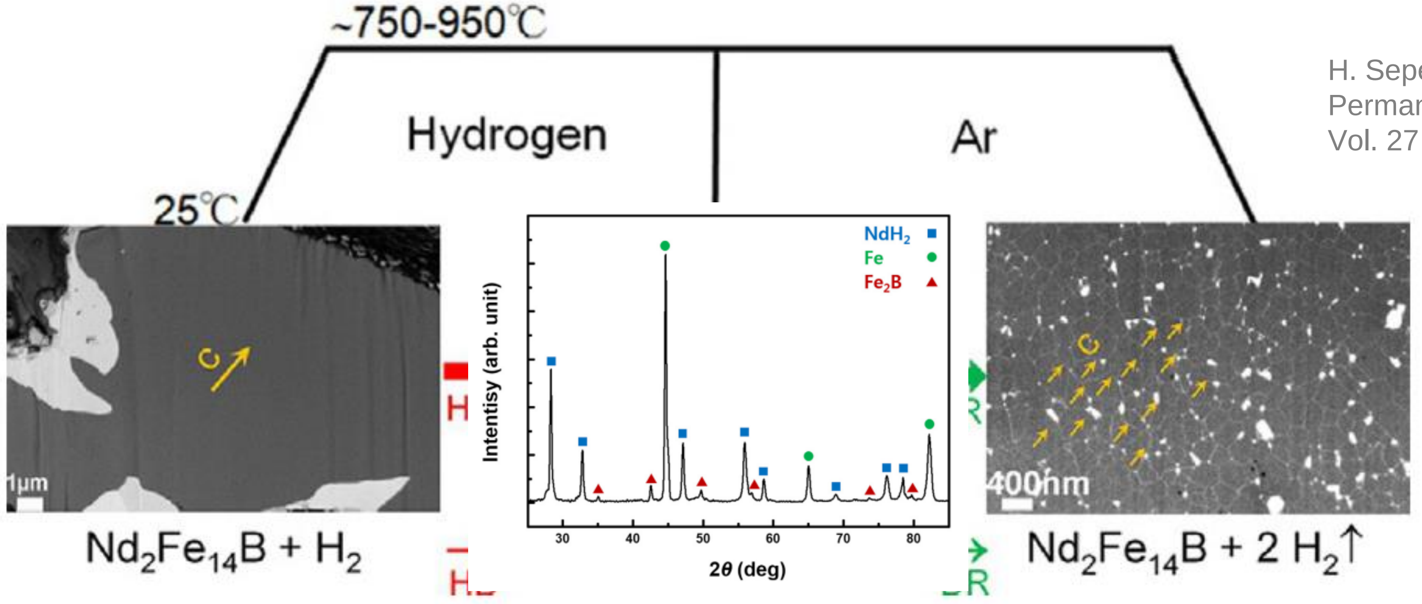

H. Sepehri-Amin et al., Advances in Nd-Fe-B Based Permanent Magnets, Handbook of Magnetic Materials, Vol. 27 (2020)

Nanosize powders

FIG. 4 Schematic of hydrogenation disproportionation desorption recombination process of Nd-Fe-B based powders.

- Starts: Mono-crystalline 2:14:1 powders prepared crushed ingot
- HD: Nd rich grain boundary absorbs H → forms NdH_2 → volume expension →Bulk material decrepitate → Single-crystalline nanosized powders
- DR: Powders AN in Ar to recombines all these phases → ultra fined grained $Nd_2Fe_{14}B$.

HDDR:

Case study: $Nd_{12.8}Fe_{80.1}B_{6.6}Ga_{0.3}Nb_{0.2}$ (Co,Ga,Nb and Zr) → For crystallographic texture development

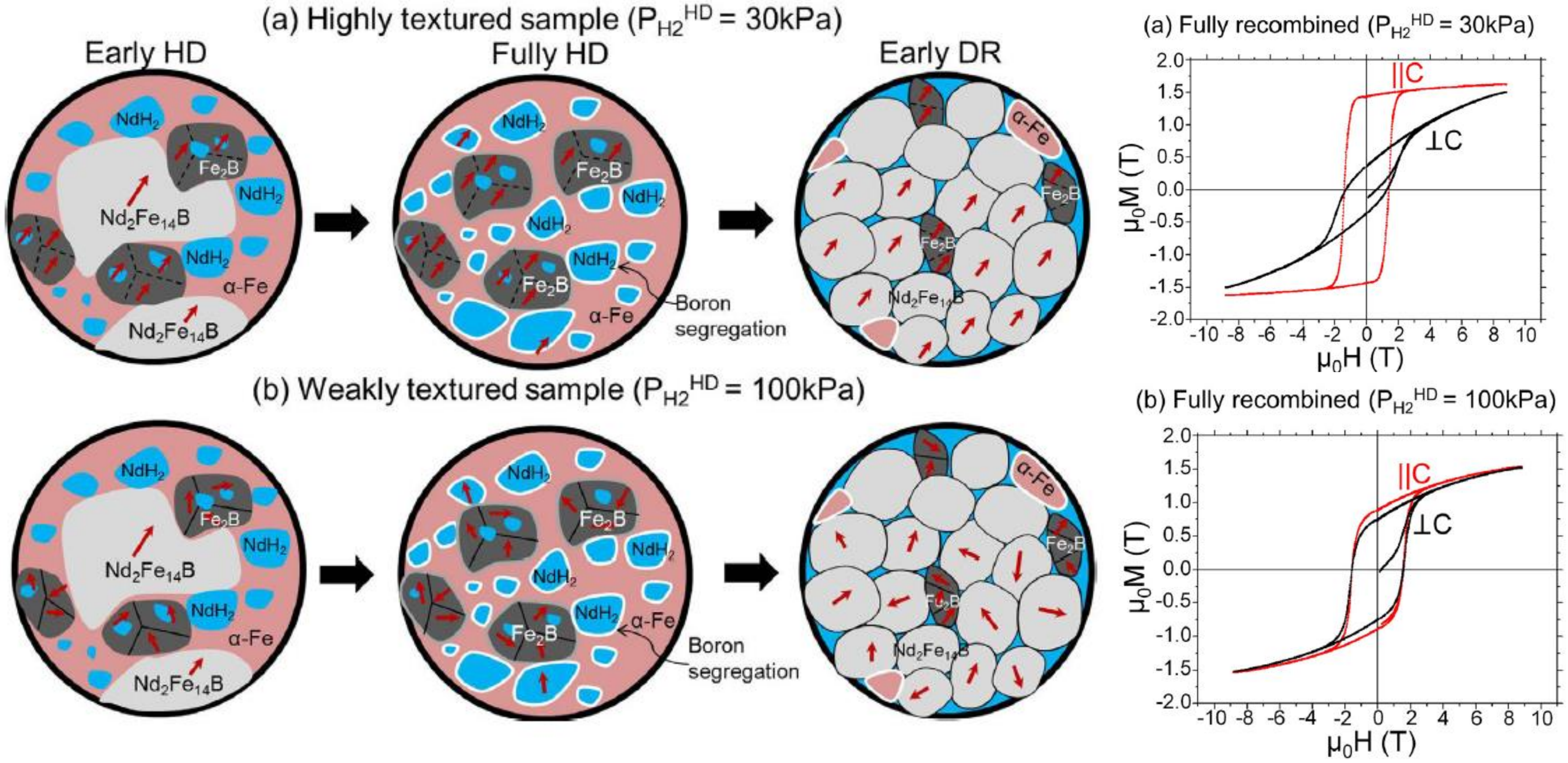

30kPa: Fe2B phase has a direct crystallographic orientation relationship with the initial $Nd_2Fe_{14}B$ grains

H. Sepehri-Amin et al., Acta Mater, 85 (2015) 42–52

Processing routes:

TECHNISCHE UNIVERSITÄT DARMSTADT

Sintered magnet:

$Fe_{76}Nd_{13.5}Pr_{0.2}Dy_{0.2}Tb_{0.2}B_{6.6}Cu_{0.1}Al_{0.5}Ni_{0.4}Co_{1.8}O_{0.5}$ **$(BH)_{max}$=400 kJ/m^3** μ_0M_r =1.46 T μ_0H_c =1.24 T

HDDR:

Textured resin bonded magnet:

$Nd_{12.6}Fe_{69.3}Co_{11.6}B_{6.0}M_{0.5}$ M=Ga,Zr,Nb,Ta,Hf (M for texture) **$(BH)_{max}$=144 kJ/m^3** μ_0M_r =0.89 T μ_0H_c =1.37 T

Hot pressing of anisotropic powders

$Nd_{12.6}Fe_{69.3}Co_{11.6}B_{6.0}M_{0.5}$ M=Ga,Zr,Nb,Ta,Hf (M for texture) **$(BH)_{max}$=271 kJ/m^3** μ_0M_r =1.25T μ_0H_c =1.08 T

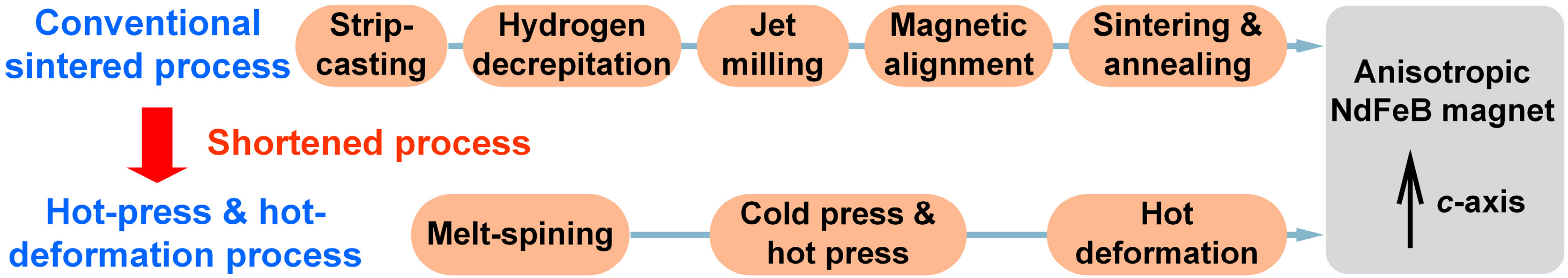

Hot deformation:

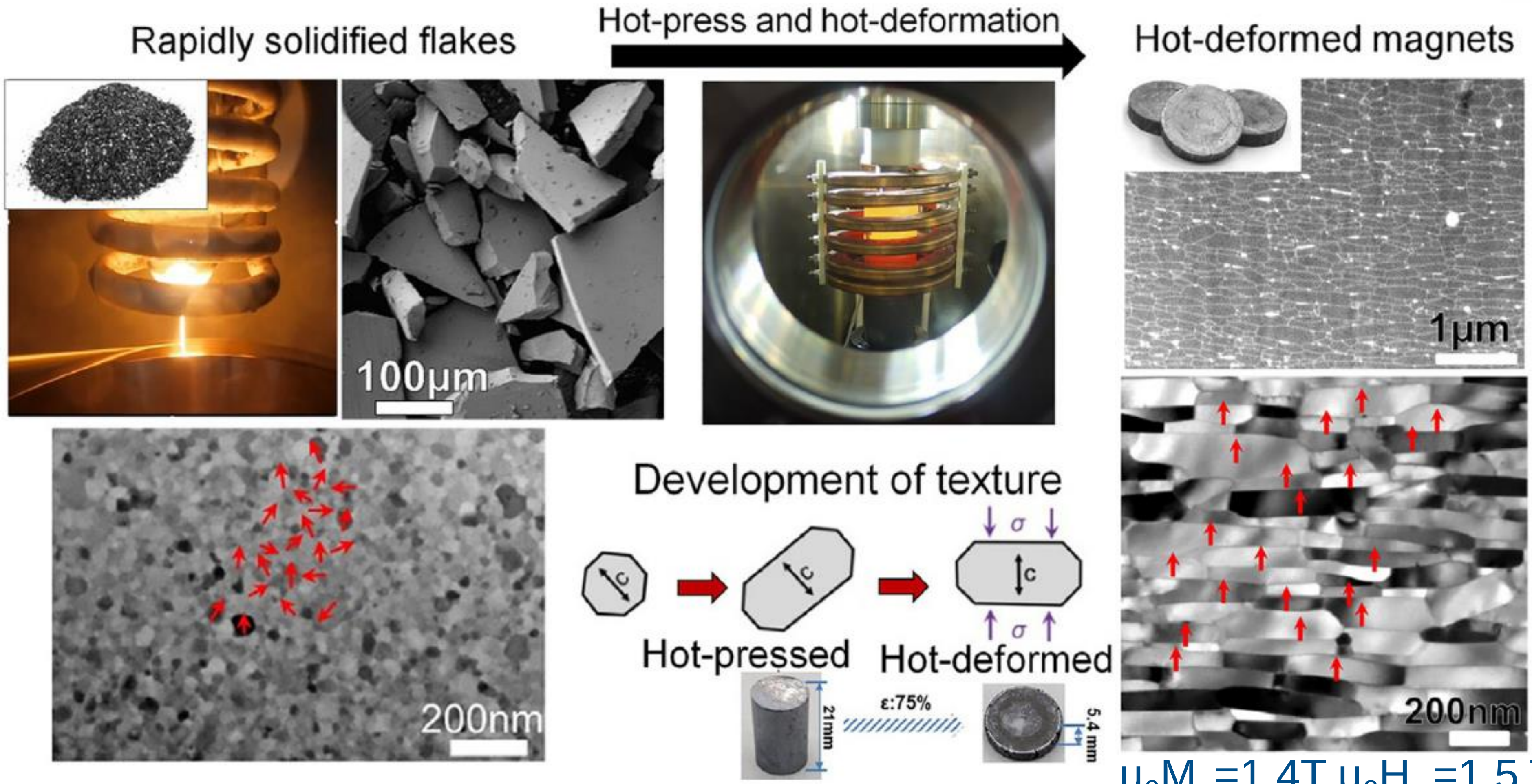

FIG. 3 Schematic illustration of development of anisotropic hot-deformed Nd-Fe-B magnets.

$\mu_0 M_r$ =1.4T $\mu_0 H_c$ =1.5 T

Anisotropic grain growth of $Nd_2Fe_{14}B$ nanocrystals in rapidly solidified alloys along the c-plane and the rotation of the grown platelet-shaped crystallites during plastic flow.

H. Sepehri-Amin et al., Advances in Nd-Fe-B Based Permanent Magnets, Handbook of Magnetic Materials, Vol. 27 (2020)

Nd-Fe-B based magnets for applications:

TECHNISCHE UNIVERSITÄT DARMSTADT

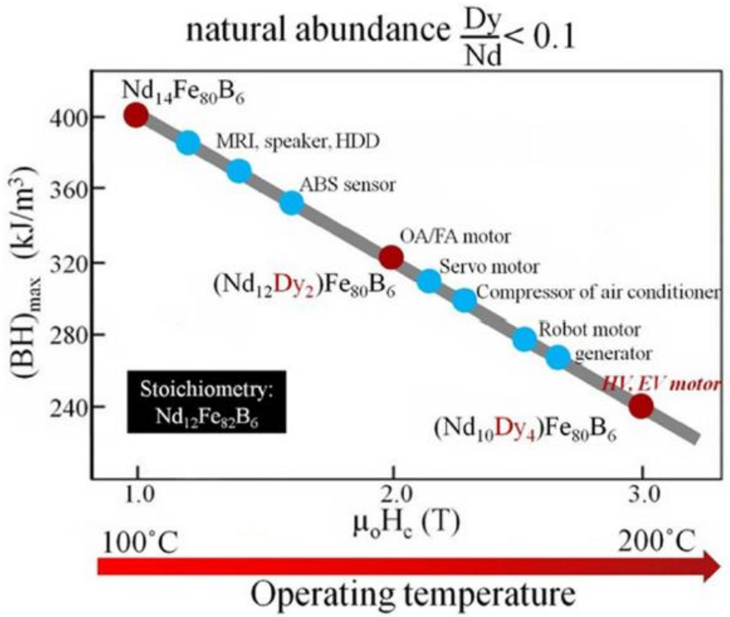

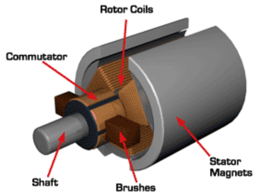

	$\mu_0 M_s$ (T)	$\mu_0 H_a$ (T)	T_C (K)
$Nd_2Fe_{14}B$	1.61	7.5	586
$Dy_2Fe_{14}B$	0.71	15	598

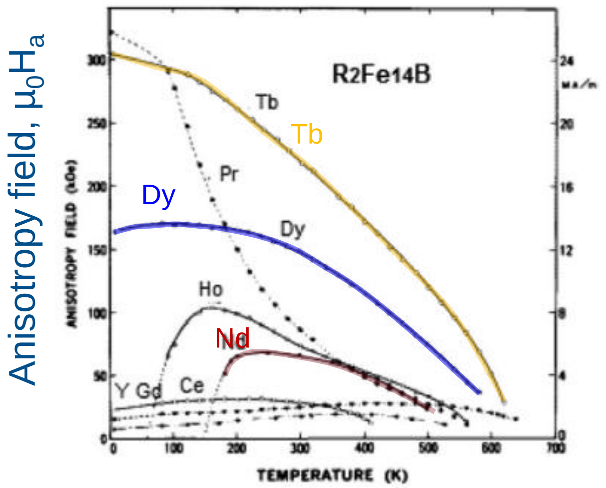

Operating temperature above 150 ºC, part of Nd must be substituted with Dy or Tb. This impacts directly the coercivity of the magnet which represents its resistance to demagnetization.

[1] H. Sepehri-Amin et al. Handbook of magnetic materials, 269-372.(2018)
[2] S. Hirosawa et al. J. Appl. Phys. 59, 873 (1986)

Sintered magnet:

$Fe_{76}Nd_{13.5}Pr_{0.2}Dy_{0.2}Tb_{0.2}B_{6.6}Cu_{0.1}Al_{0.5}Ni_{0.4}Co_{1.8}O_{0.5}$ **$(BH)_{max}$=400 kJ/m^3** $\mu_0 M_r$ =1.46 T $\mu_0 H_c$ =1.24 T

TECHNISCHE
UNIVERSITÄT
DARMSTADT

But:

Critical elements

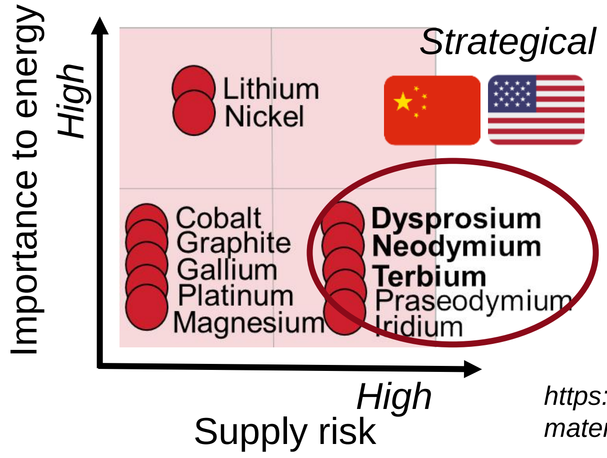

Climate goals 2050: Economy with net-zero greenhouse gas emission

https://www.energy.gov/cmm/what-are-critical-materials-and-critical-minerals

Green energy application

Wind turbines

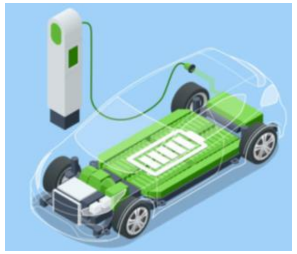

Electric car

Production

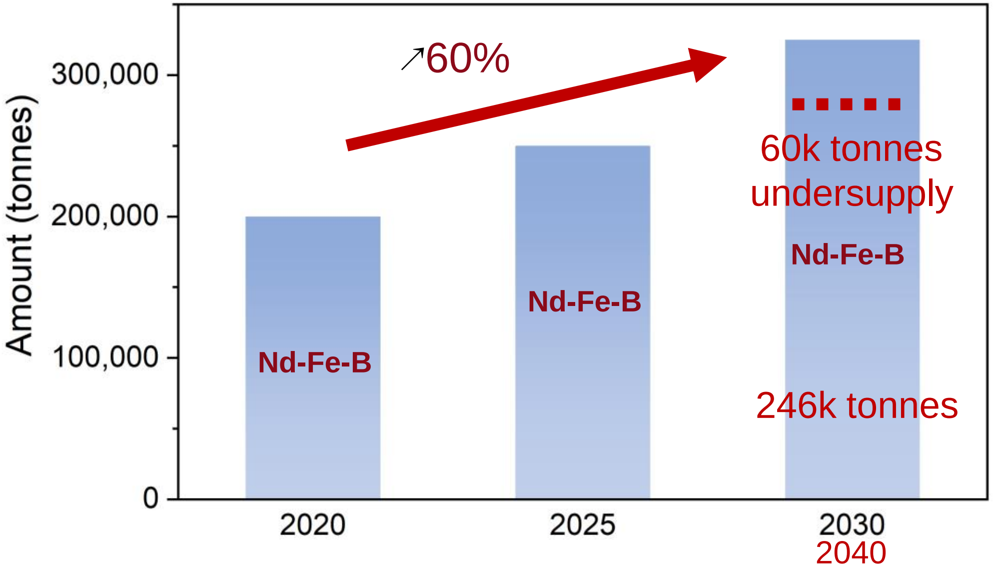

Adams Intelligence
Grand View Research

Directions:

- Decreasing HRE content

Grain boundary diffusion

- Utilization of abundant rare earth La, Ce
- Without HRE
- Recyling of NdFeB magnets
- Developing a new **Resource-efficient magnet:** Secure, affordable, sustainable.

Challenge: No new magnet for the last 35 years!

Grain boundary diffusion:

Dy-free magnet

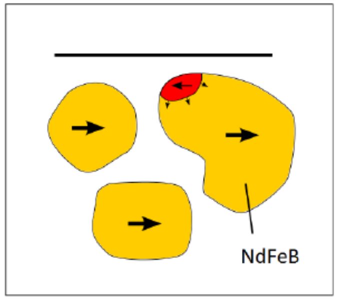

- reduced magnetic anisotropy at grain boundaries
- nucleation of reversed domains in low magnetic fields
- low coercivity

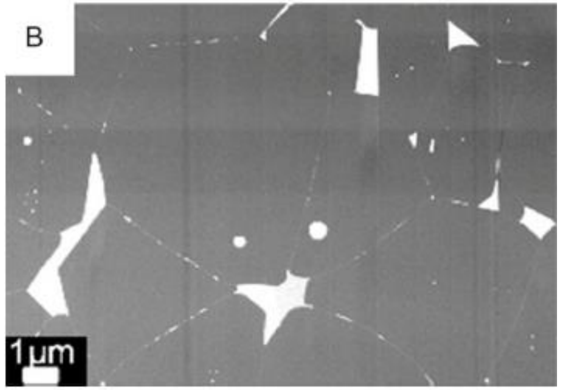

Conventional magnet with Dy

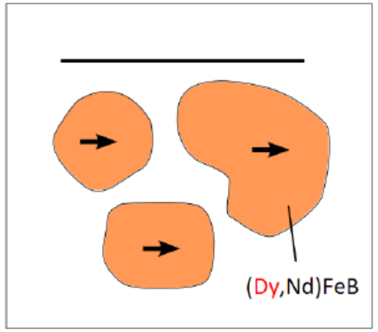

- Dy added to precursor
- homogenous Dy distribution in grains
- high coercivity
- high amount of Dy

Dy as GBDP

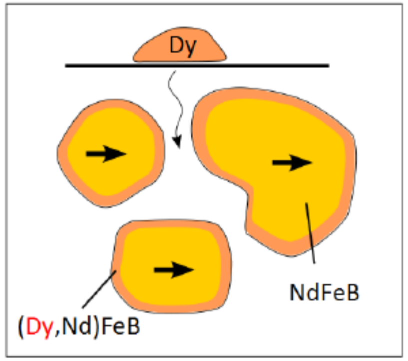

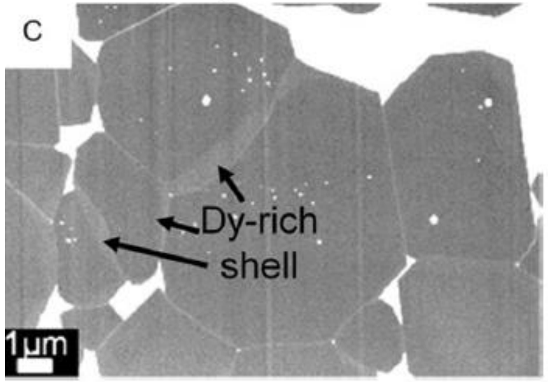

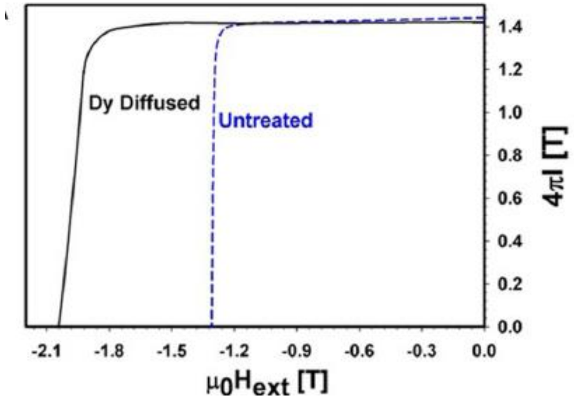

Dy content can be decreases ≈50-70%.

Löwe et al. Acta Mater. 83 (2015) 248-255
H. Sepehri-Amin et al. Acta Mater. 61 (2013) 1982

Grain boundary diffusion: Without RE

TECHNISCHE UNIVERSITÄT DARMSTADT

$Nd_{14}Fe_{76}Co_{3.4}B_6Ga_{0.6}$ (at.%) + $Nd_{70}Cu_{30}$ GBD

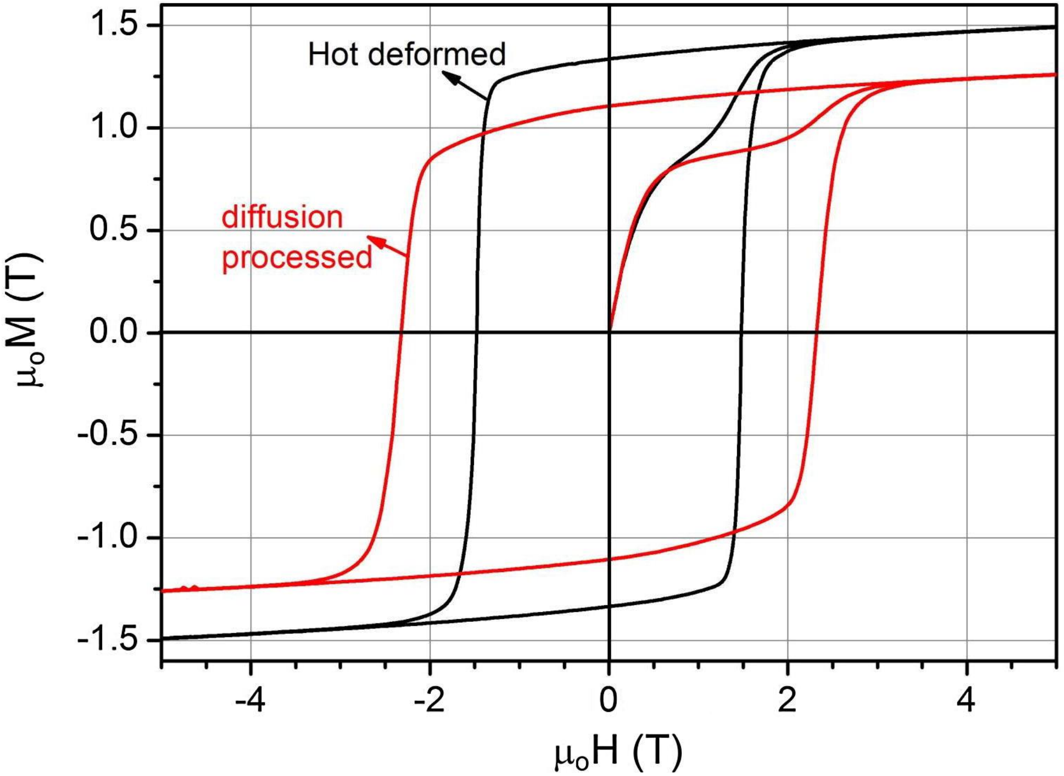

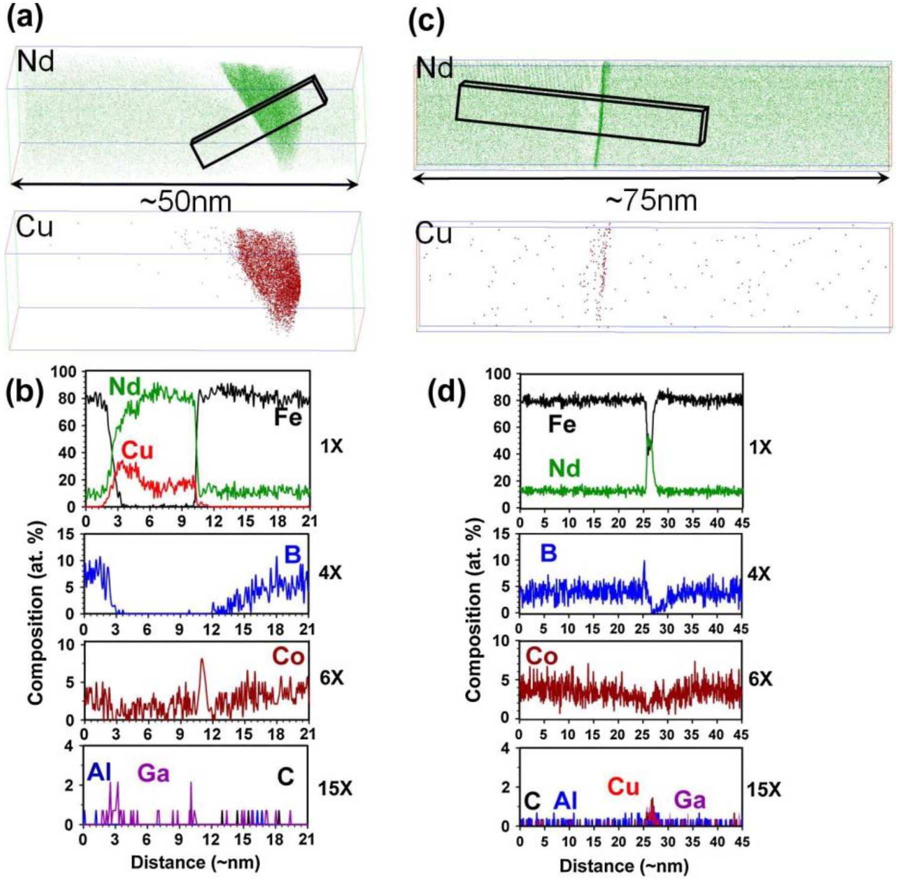

The intergranular phase of the hot-deformed magnet initially contained ~55 at.% ferromagnetic element, while it diminished to an undetectable level after the process

H. Sepehri-Amin et al., Acta Mater. 61 (17) (2013), 6622-6634.

Developing $SmFe_{12}$-magnet:

High anisotropy (H_a)
Magnetization (M_s)

+

Optimum microstructure
Intergranular phase

→

High coercivity (H_c)
Remanence (M_r)

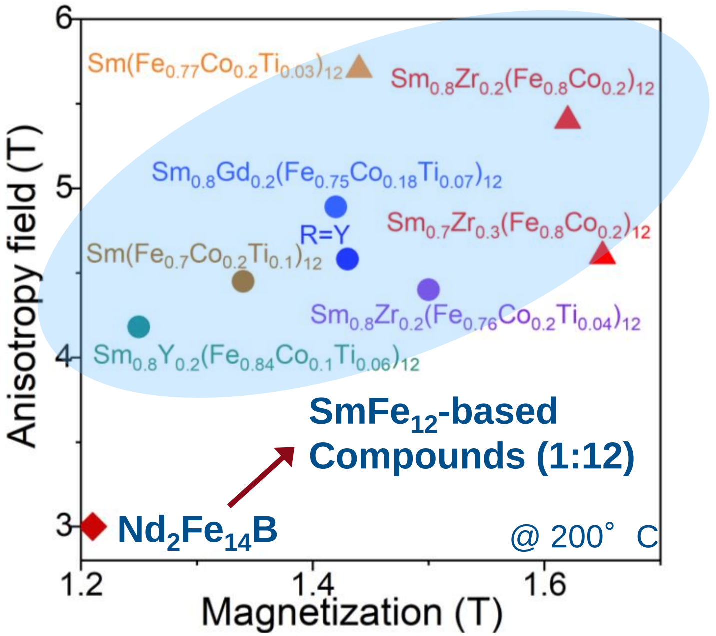

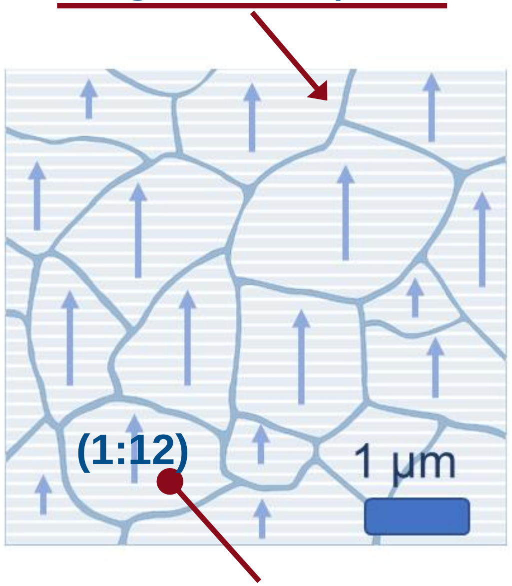

Fine magnetic grains

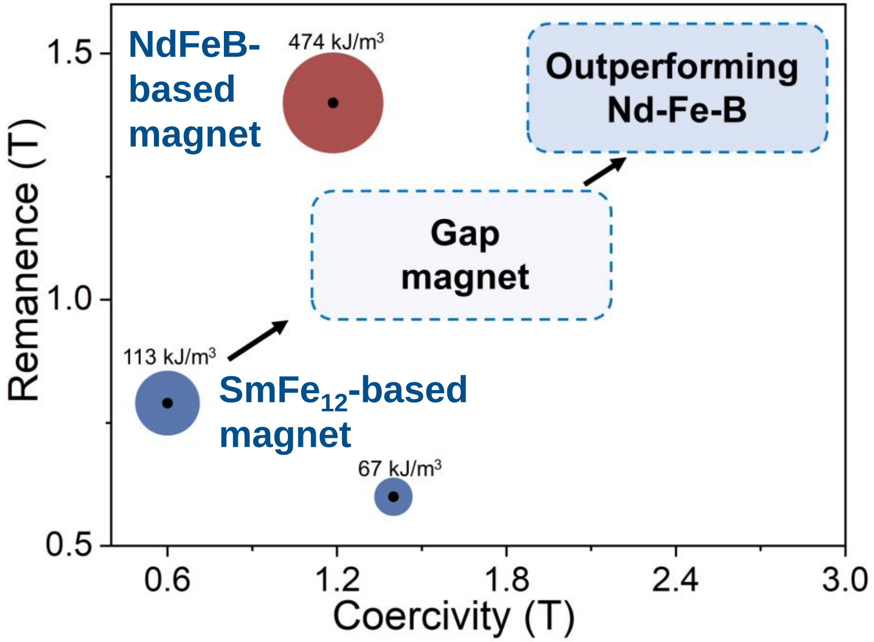

[1] **P. Tozman** et al. Acta Mater. 153 (2018)
[2] **P. Tozman** et al. Scr. Mater., 194 (2021)

Phase diagram:
Magnetic $SmFe_{12}$ + low melting point phases

Bringing to the physical limit
$H_c \geq 30\% H_a$
$M_r \geq 90\% M_s$

Advertisements:

TECHNISCHE UNIVERSITÄT DARMSTADT

https://magnetism.eu/271-recordings-2024.htm#par2356

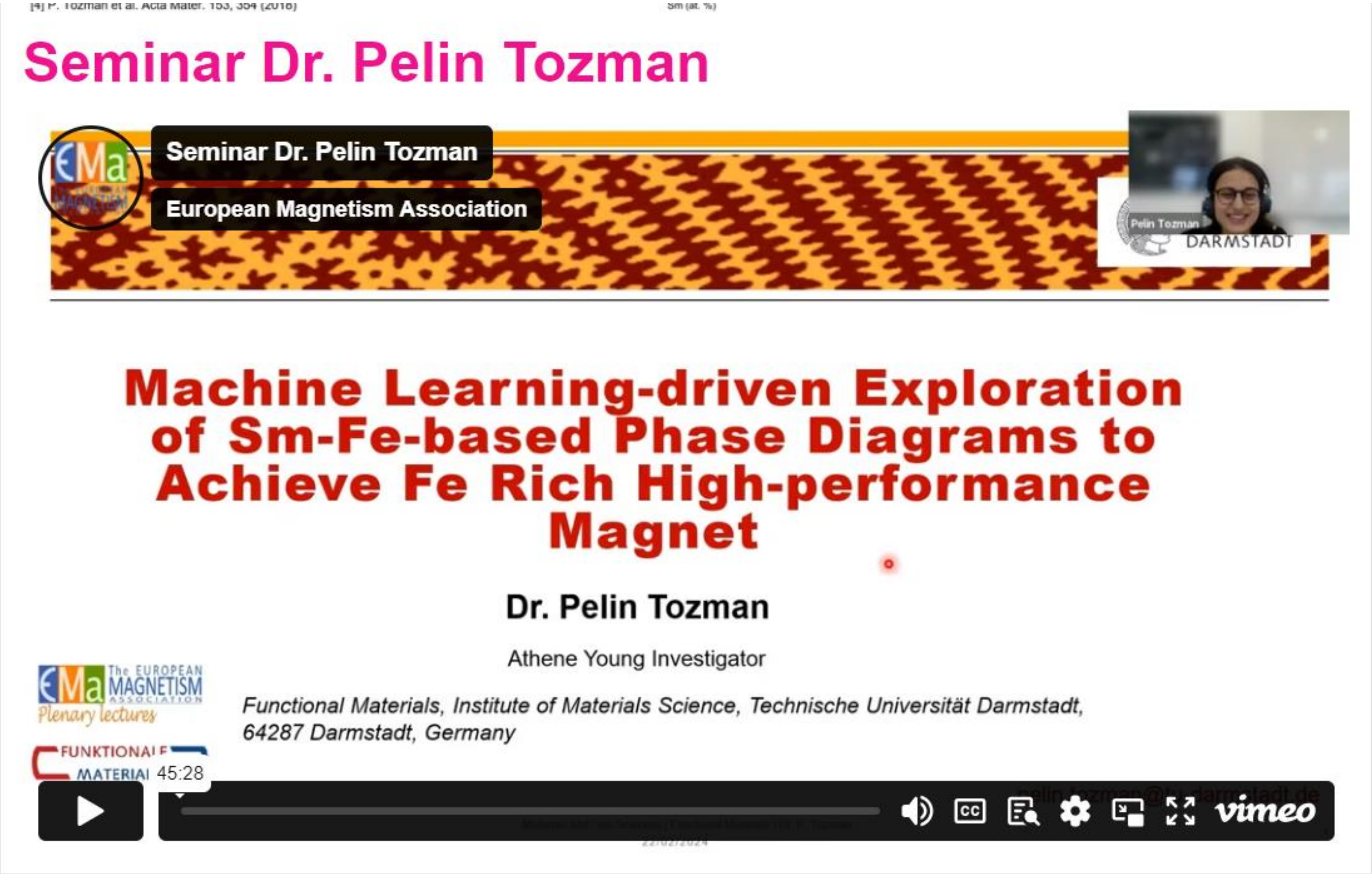

Advertisements:

TECHNISCHE UNIVERSITÄT DARMSTADT

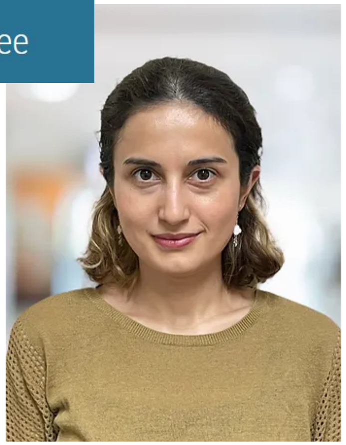

Invited speaker AtC-AtG 2024

Pelin Tozman

Technical University of Darmstadt, Germany

Region: Europe, Middle East and Africa

Field: Multi-Functional Magnetic Materials and Applications

Presentation title

Development of magnetic recording strategies: A journey from magnetic tape to multi-level heat-assisted magnetic recording

Pelin Tozman is Athene Young Investigator Fellow in Functional Material group in Technical University of Darmstadt, Germany. She got her PhD from Trinity College Dublin and she worked as a ICYS research fellow in Research Center for Magnetic and Spintronic Materials group in National Institute for Materials, Tsukuba. Her research cover various areas of magnetism such as developing novel materials for practical applications; permanent magnet for green energy technology, magnetic recording media for hard disk drives, spintronic applications, and noise suppression materials for 5G communication. For this purpose, she worked on different types of compositions, in various forms (nanocomposite, nano powders, ingot, thin-film, nanofabrication).

Acknowledgement:

We are hiring…

Technical University of Darmstadt,
Functional Materials
Prof. Dr. Oliver Gutfleisch
Dr. Pelin Tozman

https://www.mawi.tu-darmstadt.de/fm/group_members_fm/jobs_fm/application_form.en.jsp

pelin.tozman@tu-darmstadt.de

Master students:
Maria Takeuchi
Aaron D. Zamalloa
Giray Erdem
Eren Foya
Konstantinos Grammatikakis

Funding:
Athene Young Investigator
(2023-2026)

THANKS FOR LISTENING